Journal of Chemical Physics

Submitted December 28, 2023

Revised January 22, 2024

Adiabatic Ionization Energies of RuC, RhC, OsC, IrC, and PtC

Dakota M. Merriles, Yexalen Barrera-Casas, Annie S. Knapp,[a)] and Michael D. Morse[b)]

Department of Chemistry

University of Utah

Salt Lake City, Utah 84112

a) Current address: Department of Chemistry, Yale University, 225 Prospect Street, PO Box 208107, New Haven, CT 06520-8107

[b)]Author to whom correspondence should be addressed: morse@chem.utah.edu

ABSTRACT

The ionization energies (IEs) of RuC, RhC, OsC, IrC, and PtC are assigned by the measurement of their two-photon ionization thresholds. Although late transition metal-carbon bonds are of major importance in organometallic chemistry and catalysis, accurate and precise fundamental thermochemical data on these chemical bonds is mainly lacking in the literature. Based on their two-photon ionization thresholds, in this work we assign IE(RuC) = 7.439(40) eV, IE(RhC) = 7.458(32) eV, IE(OsC) = 8.647(25) eV, IE(IrC) = 8.933(74) eV, and IE(PtC) = 9.397(32) eV. These experimentally derived IEs are further confirmed through quantum chemical calculations using coupled-cluster single double perturbative triple methods that are extrapolated to the complete basis set limit using a three-parameter mixed Gaussian/exponential extrapolation scheme and corrected for spin-orbit effects using a semiempirical method. The electronic structure and chemical bonding of these MC species are discussed in the context of these ionization energy measurements. The IEs of RuC, RhC, OsC, and IrC closely mirror the IEs of the corresponding transition metal atoms, suggesting that for these species, the (n+1)s electrons of the transition metals are not significantly involved in chemical bonding.

I. INTRODUCTION

The transition metal-carbon bond is of fundamental interest in organometallic, inorganic, and materials chemistry.[1-7] Transition metal-carbon based complexes are prevalent in a variety of chemical domains, and their profound importance in the sciences has been recognized by a number of Nobel Prizes.[8-10] Studies of the fundamental properties of the transition metal-carbon chemical bond are worthy endeavors and have been the focus of numerous spectroscopic and computational works over the past several decades. The simplest and most straightforward systems for probing the electronic and thermochemical properties of the transition metal-carbon bond are the diatomic transition metal carbide molecules, MC. To the best of our knowledge, all of the group 3-10 transition metal monocarbide molecules have had their electronic ground states and bond lengths experimentally assigned and measured, except for MnC, TcC, HfC, and ReC.[11-30] Also heavily investigated, both experimentally and computationally, are the bond dissociation energies (BDEs) of the open *d*-subshell MC molecules and their cations.[31-49] One of the last relatively uncharted frontiers for elucidating the fundamental properties of the MC molecules is the precise measurement of their adiabatic ionization energies (IEs). These are fundamental thermochemical quantities that relate the thermochemistry of the neutral molecule to that of the cationic form.

Spectroscopically measuring accurate and precise IEs for MC species allows for additional information to be extracted about the molecule itself as well as allowing the consistency of previous measurements to be gauged. This may be accomplished through the thermochemical cycle:

$$D_0(MC) + IE(M) = IE(MC) + D_0(M^+\text{-}C), \quad (1.1)$$

where $D_0(MC)$ is the BDE of the neutral MC molecule, IE(M) is the IE of the transition metal atom, IE(MC) is the IE of the neutral MC molecule, and $D_0(M^+\text{-}C)$ is the BDE of the MC^+ cation. Eqn. 1.1 shows that when three of those values are known, the fourth value can be derived. When all four values are experimentally known, Eqn. 1.1 provides a check for self-consistency. As implied above, it is the ionization energies of the MC molecules, IE(MC), that are least well-studied among the four quantities of

Eqn 1.1. Prior to the current work, the most useful measurements of IE(MC) values are for TiC,[12] VC,[50] FeC,[51] CoC,[52] NiC,[53] NbC,[21] and PtC.[54] Using Eqn 1.1, BDEs for neutral and cationic MCs have allowed the IEs of ScC, YC, ZrC, LaC, HfC, and TaC to be previously derived by our group.[31, 32] Appearance potentials of several of the MC^+ ions are known from Knudsen effusion mass spectrometry, but the error limits assigned to these values can be as large as 1 eV.[39, 55, 56] An error limit this large precludes the elucidation of periodic trends and greatly reduces their utility when employed in Eqn 1.1. Other than the previously noted experimental value for IE(PtC),[54] measured IEs of useful precision are generally lacking for the late 4d and 5d family of transition metal monocarbides. In the present work, we provide new, accurate, and precise IE values for RuC, RhC, OsC, IrC, and PtC. These IE values help to elucidate the thermochemistry of these MC molecules while providing benchmarks for quantum chemical calculations as well. Moreover, the ionization energies of these molecules also contribute towards the construction of a comprehensive database of thermochemical properties of late transition metal molecules.[57, 58]

In recent years, computational chemistry has greatly benefited from the increased availability of accurately measured thermochemical data, especially for the open *d*- and *f*-shell molecules, which are innately challenging subjects for computational chemistry.[59-64] These new experimental measurements allow rigorous testing of computational methods according to a variety of experimentally-verified standards. The premise of a global "experimental accuracy" standard for quantum chemical calculations was first proposed by Pople in his 1998 Nobel lecture on quantum chemical methods.[65] The standard proposed by Pople for calculations involving main group elements is 1 kcal/mol (about 0.04 eV). In other words, a quantum chemical computational method should seek to predict energetic properties of main-group compounds to an accuracy of 1 kcal/mol or better. Because of the challenges associated with calculating transition metal compounds and the overall paucity of precise experimental data on these compounds, a relaxed experimental accuracy standard of 3 kcal/mol (about 0.13 eV) for molecules containing transition metals has been suggested.[66] The IEs of RuC, RhC, OsC, IrC, and PtC reported in

the present investigation easily meet this requirement and are therefore suitable benchmarks for computational chemistry.

II. EXPERIMENTAL

The spectrometer used to measure the two-photon ionization thresholds of RuC, RhC, OsC, IrC, and PtC is the same instrument that was most recently used to measure the IEs of the late MB molecules.[57] The spectrometer is separated into two chambers, the source chamber and the analytical chamber. The molecules of interest are synthesized *in situ* in the source chamber, where they are produced in a laser ablation source that employs a stainless-steel block with two intersecting channels. The first channel, termed the reaction channel, sits on-axis with a pulsed solenoid gas nozzle. The second channel, termed the vaporization channel, intersects the reaction channel at right angles and provides a path for the light emitted by the ablation laser to be focused onto a rotating and translating metal sample disk. The production of the molecules of interest in these experiments begins with the admission of a pulse of high-pressure He gas (~120 psi) seeded with 4% CH_4 into the reaction channel to produce the transition metal carbide molecules. For RuC and IrC, experiments were also performed that used a reactant 2.5% CH_4 and 25% Ar seeded in the He gas mix to try to further cool the molecules (see Section IV). Shortly after the pulsed nozzle is fired, a pulse of laser light (Nd:YAG 2ω, 532nm, ~ 5ns, ~10mJ) is focused down the vaporization channel, traveling past the intersection with the reaction channel, irradiating the surface of a metal sample disk. For these experiments, the metal disk consisted of pure samples of Ru, Rh, Ir, and Pt that were used to produce RuC, RhC, IrC, and PtC, respectively. A V:Os (45:55) sample disk was employed for the OsC experiments.

The focused, high-power light (~10^{10} W/cm^2) produces a reactive, outwardly expanding gaseous plasma consisting of metal atoms, metal ions, and electrons. The plasma continues expanding through the vaporization channel until it reaches the intersection with the reaction channel, where a portion of the plasma is entrained in the pulsed gas flowing down the reaction channel. Here, the molecules of interest

are produced as the gaseous metal-containing plasma reacts with the seeded CH_4 gas. Although one might expect hydrogenated metal carbide molecules (MCH, MCH_2, and MCH_3) would also be produced along with MC, there is no evidence in the mass spectra for any of these species being formed. Thus, we are convinced that the measurements reported here pertain solely to the diatomic MC molecules. The metal carbide molecules are collisionally cooled by the high-pressure He gas as they continue flowing down the reaction channel for about 1 cm, subsequently expanding into the low-pressure (10^{-5} Torr) source chamber. As the products leave the high-pressure environment of the reaction channel and enter the source chamber, they undergo a supersonic expansion, cooling their rotational degrees of freedom to below 30 K.[67] The products continue propagating forward and expanding in all directions until they reach a 1 cm diameter skimmer. As the molecules move through the skimmer and enter the analytical chamber (10^{-6} Torr) a loosely collimated molecular beam is formed.

As the molecules pass through the analytical chamber, they enter the two-stage acceleration region of a Wiley-McLaren ion source.[68] There, the molecular beam is irradiated by a counterpropagating laser pulse produced by a tunable optical parametric oscillator laser (OPO). If the molecule of interest has an allowed vibronic transition that matches the wavenumber of the OPO laser, a fraction of the molecules will absorb the light and be placed in the excited vibronic level. If the excited state so produced lies more than halfway to the ionization limit, absorption of a second photon from the same laser pulse can cause ionization, which is followed by detection in the time-of-flight mass spectrometer (TOFMS). If the initially excited level lies below half the ionization energy, however, absorption of a second photon is insufficient for ionization and a three-photon ionization process is required. By adjusting the intensity of the OPO laser radiation using filters, it is possible to reduce the three-photon ionization process to tolerable levels while still easily observing ions produced by the two-photon process at higher energies, as was demonstrated in our previous report of the ionization energies of RuB, RhB, OsB, IrB, and PtB.[57]

The TOFMS consists of a drift tube that the ionized species traverse, reaching a reflectron assembly that reflects the ions down a second flight tube to a dual microchannel plate detector. Ionized

species of different masses impact the detector at different times, allowing a mass spectrum to be generated by recording ion signal as a function of time of flight. Multiple mass species can be monitored concurrently as the OPO laser scans through a defined range of wavelengths, allowing mass-resolved optical spectra to be recorded.

All the pulsed devices employed in this experiment are timed relative to a master oscillator operating at 10 Hz, so that each experimental cycle takes 100 ms to complete. The cycle begins with the pulse of high-pressure gas and concludes with digitization of detector signal, which is then stored on the data collection computer. In these studies, the OPO laser is scanned to higher photon energies in increments of 0.05 nm, with 30 experimental cycles averaged at each wavelength increment. This is sufficient for an acceptable signal-to-noise ratio to be obtained. When the two-photon ionization threshold of the molecule is identified and conditions are adjusted to optimize the signal, particularly the discrimination between two- and three-photon ionization processes, multiple scans across the same set of laser wavelengths are repeated to obtain an averaged spectrum in the vicinity of the two-photon ionization threshold. The averaged spectrum is calibrated to concurrently collected atomic transitions of the transition metal constituents that have been precisely reported by NIST.[69] In those cases where the metal of interest displays too few atomic transitions or if the atomic transitions are poorly resolved, a sample of another metal is instead employed to collect atomic transitions for calibration in a separate scan.

III. COMPUTATIONS

All quantum chemical calculations in this work employed the Gaussian 16 software suite.[70] Geometry optimizations for the $RuC^{0/+}$, $RhC^{0/+}$, $OsC^{0/+}$, $IrC^{0/+}$, and $PtC^{0/+}$ molecules were performed with the unrestricted B3LYP density functional[71] using ground state spin multiplicities that have been previously reported in the literature for each molecule.[23, 28, 29, 72, 73] The all-electron augmented correlation-consistent aug-cc-pVQZ[74, 75] basis set was employed for the carbon atom and the appropriate relativistic energy-consistent pseudopotentials and their augmented correlation-consistent basis sets of quadruple zeta

quality (aug-cc-pVQZ-PP)[76, 77] were employed for Ru, Rh, Os, Ir, and Pt in these geometry optimizations.

After the optimized geometries and ground electronic states (*i.e.*, molecular orbital (MO) occupancies) of each molecule were confirmed, extrapolation to the complete basis set limit (CBSE) was achieved using single-point coupled-cluster single double perturbative triple [CCSD(T)] energy calculations for each molecule using the optimized geometries and MO occupancies. The CBSE was done by performing three different CCSD(T) calculations on each molecule with different quality basis sets and the resulting energies were fit to a three-parameter mixed Gaussian/exponential extrapolation scheme:[78, 79]

$$E(n) = E_{CBS} + Ae^{-(n-1)} + Be^{-(n-1)^2} \quad (3.1)$$

This was solved using n = 3, 4, and 5, with E(n) representing the CCSD(T) single-point energies using the aug-cc-pVXZ(-PP) (X = 3, 4, 5) family of basis sets, respectively. In a previous work on the IEs of late MB species, this CCSD(T)/CBSE methodology gave calculated IEs in good agreement with the measured IEs.[80] All of the basis sets used in this work were obtained from the Basis Set Exchange.[81] Zero-point energy corrections were also included, based on the B3LYP calculated vibrational frequencies.

Spin-orbit effects influence the energetics of transition metal compounds, and this includes their IEs as well. Explicitly accounting for spin-orbit effects in these calculations is beyond the scope of the current work, however. Estimates of spin-orbit effects for molecules with ground electronic states that have $\Lambda > 0$ can be obtained using first-order perturbation theory, however.[37, 57, 58] In this study, OsC, IrC, RuC^+, and OsC^+ all have nonzero orbital angular momenta in their ground electronic states. As further detailed in the Supplementary Information, semi-empirical spin-orbit stabilization corrections can be estimated for these molecules. An in-depth derivation of how these first-order spin-orbit corrections are estimated has been previously described.[37] Using this procedure, we obtain first-order spin-orbit stabilization corrections of -0.378 eV, -0.129 eV, and -0.378 eV for OsC, RuC^+, and OsC^+, respectively. Clearly, OsC and OsC^+ have the same estimated spin-orbit correction, so its adiabatic IE will remain unchanged. Cationic RuC^+, however, is stabilized by 0.129 eV, lowering the calculated adiabatic IE by that much for the RuC molecule. The spin-orbit splitting between the $\Omega = 5/2$ and $\Omega = 3/2$ components of

the IrC $^2\Delta$ ground state was thought to be experimentally known to be 0.397 eV,[29] but upon later examination, it was found that the authors of that work were actually resolving the energy difference between the $^2\Delta_{5/2}$ ground electronic state of IrC and its low-lying $^2\Sigma^+$ excited state.[82] Because the spin-orbit splitting of the IrC $^2\Delta_{5/2}$ ground state has yet to be measured, we instead apply the estimated spin-orbit correction of 0.448 eV directly to the calculated IE of IrC. See the Supplementary Information for more details on the first-order spin-orbit corrections applied here.

IV. RESULTS

The measured two-photon ionization thresholds in the resonant two-photon ionization (R2PI) spectra of RuC, RhC, OsC, IrC, and PtC are displayed in Figures 1-5, respectively. At photon energies that are less than half of the IE ($\nu < ½$ IE(MC)), the absorption of two photons cannot ionize the molecule, so the only ion signal that can be detected results from the absorption of three photons. The laser intensity is insufficient to allow three-photon processes to occur readily, so baseline prevails in this region. When the photon energy exceeds IE/2, however, two-photon ionization processes become possible, and an R2PI spectrum is observed. For all five of the investigated molecules, there is a high density of vibronic states in the vicinity of IE/2, so a discrete but congested R2PI spectrum is seen. The high density of closely spaced vibronic levels in the vicinity of IE/2 allows the two-photon ionization threshold to be assigned with relatively small error limits. A potentially important consideration is that due to the high density of states, spin-orbit interaction is expected to lead to molecular eigenstates in the vicinity of IE/2 that have poorly defined values of total spin, so that spin-based constraints on the ionization step are not expected to be present. Likewise, spin-orbit and nonadiabatic interactions are expected to severely mix the vibronic states in this region, leading to vibrational amplitude that spans a broad range of internuclear separations. We anticipate that this will lead to a diminished importance of Franck-Condon effects in the ionization step. The absence of significant spin selection rules and Franck-Condon constraints in the ionization step in this R2PI process is a potential advantage for measuring IEs as compared to a direct one-photon

process, where the lack of state mixing in either the ground state of the neutral or of the cation can lead to strong spin selection rules and Franck-Condon effects.

To convert the measured two-photon ionization threshold to the adiabatic IE, the two-photon ionization threshold is simply doubled. However, our measurements are performed in a static electric field in the Wiley-McLaren ion source. Thus, the ionization energy is shifted to lower energies by the field ionization effect. In a previous study of atomic lanthanum, we have measured the field ionization shift for ionization of the ground $^2D_{3/2g}$ and spin-orbit excited $^2D_{5/2g}$ states of La to be 52 ± 20 cm^{-1}.[57] Accordingly, the adiabatic IE is obtained by doubling the two-photon ionization threshold (and its error limit) and adding the field ionization shift to this value.

Error limits ranging from 200 cm^{-1} to 600 cm^{-1} are assigned to the ionization energies of the MC molecules studied here. The assigned error limits encompass the linewidth of the OPO laser (<10 cm^{-1}), the average rotational energy of the molecules (<20 cm^{-1}), and the errors in the calibration of the atomic transitions to the values listed in the NIST Atomic Spectral Database (<5 cm^{-1}).[69] The largest contribution to the error, however, arises from the density of vibronic levels in the region near IE/2. When a highly congested vibronic spectrum is observed just above the two-photon ionization threshold, as found in Figure 3 for OsC, the threshold can be identified with little uncertainty, leading to an assigned error limit in the location of the two-photon ionization threshold for OsC of ±90 cm^{-1}. This is indicated by the horizontal bar atop the arrow specifying the two-photon ionization threshold in Figure 3. When converted to the ionization energy, this error limit is doubled and the error associated with the field ionization shift, 20 cm^{-1}, is added to it, giving an assigned error in IE(OsC) of 200 cm^{-1}. In cases where the vibronic spectrum is less congested, as in Figures 2 and 5 for RhC and PtC, respectively, a more conservative error limit is assigned, reflective of the greater average separation between vibronic levels in these molecules. For RhC and PtC, the error limit was taken by calculating the average spacing between significant vibronic features and dividing by two. The threshold was then assigned at an energy equal to the wavenumber of the red-most clearly identifiable vibronic band, minus the assigned error limit. The

rationale behind this approach is that the two-photon ionization threshold should be chosen halfway between the last unobserved band and the first observed band, with an error limit that encompasses both features. Of course, the problem is that the last unobserved band is unobserved. This method uses the observed bands to the blue of the threshold to infer the likely position of the last unobserved band. For RhC and PtC, this leads to an assigned error limit in the threshold of 120 cm^{-1} and an error limit in the IE of 260 cm^{-1}.

In the R2PI spectrum for RuC displayed in Figure 1, there is a slow rise of RuC ion signal starting around ≈29,100 cm^{-1}, below the assigned two-photon threshold at 29,975(150) cm^{-1}. Regardless of the experimental parameters used to try to cool the RuC molecules, the lingering tail of ion signal below 29,975 cm^{-1} persisted. We believe that the ion signal in this region is the result of ionization of a small fraction of the RuC molecules in the low-lying $^3\Delta_3$ and $^3\Delta_2$ electronic states. In a previous R2PI spectroscopy experiment that rotationally resolved the spectra of RuC, it was found that the low-lying $^3\Delta_3$ and $^3\Delta_2$ electronic states lie only 76 cm^{-1} and 850 cm^{-1} above the $^1\Sigma^+$ ground state, respectively.[23] The 850 cm^{-1} term energy of the $^3\Delta_2$ state correlates well with the onset of the baseline rise about 875 cm^{-1} to the red of that assigned ionization threshold, supporting this hypothesis. To the blue of the two-photon ionization threshold around 30,280 cm^{-1} and 30,448 cm^{-1} are two large dips in the RuC molecular signal. These match the wavenumbers of the two saturated transitions in the spectrum of atomic Ru shown in the lower trace. These strongly allowed atomic transitions create so many atomic ions that space charge effects cause the ion cloud to expand greatly as it traverses the time-of-flight drift tubes, greatly depleting the number of ions of all types that reach the detector. As a result, the molecular signal due to RuC^+ is nearly completely depleted. The is a known artifact of the R2PI method,[83, 84] causing these depletions in ion signal to be repeated in every scan that covered this range. Accounting for the ambiguity in precisely identifying the two-photon ionization threshold, we assign an error limit of ±150 cm^{-1} to the threshold, giving a final error limit of ±320 cm^{-1} to IE(RuC).

The most conservative error limit assigned in this study was for the two-photon ionization

threshold of IrC. Ultimately, an error limit of ±600 cm^{-1} was assigned for IE(IrC) because of ambiguities in the recorded spectrum. As displayed in Figure 4, the arrow points to the assigned two-photon ionization threshold. However, the small bumps and increases in molecular signal from 35,600 cm^{-1} to 36,200 cm^{-1} makes it difficult to discern the precise location of the threshold. Theoretical calculations on IrC predict an excited $^2\Sigma^+$ electronic state lying approximately ~400 cm^{-1} above its $^2\Delta_{5/2}$ ground state.[82] Unfortunately, this low-lying $^2\Sigma^+$ state has not yet been experimentally observed, so experimental confirmation of its term energy is not available. Nevertheless, the fact that such a low-lying electronic state has been calculated gives credence to the possibility that the weak features at the low wavenumber end of the spectrum could arise from a small population in this low-lying state, analogous to what is observed in RuC. To account for this possibility, we have assigned a relatively large error limit that encompasses this ambiguity, as shown in Figure 4. We attempted to further cool the RuC and IrC molecules by repeating the scans using a carrier gas mix of 2.5% CH_4 in He gas that was also seeded with 25% Ar. Unfortunately, even with the added argon, the two-photon ionization thresholds remained ambiguous, requiring larger error limits to be assigned for IE(RuC) and IE(IrC).

V. DISCUSSION

A. Electronic Structure of MC and MC^+ Species

The molecular orbitals (MOs) and their relative energies of $RuC^{0/+}$, $RhC^{0/+}$, $OsC^{0/+}$, $IrC^{0/+}$, and $PtC^{0/+}$ are similar to those of other diatomic late transition metal *p*-block molecules.[80] Figure 6 presents a qualitative MO diagram of these late MC molecules, using RuC in its ground $^1\Sigma^+$ state as an illustrative example. The ten valence MOs of the late MC molecules are generated from the (n+1)*s* and n*d* atomic orbitals (AOs) of the transition metal atom combined with the 2*s* and 2*p* AOs of the carbon atom. Figure 6 displays the valence MOs of the RuC molecule, numbered according to increasing energy. The 1σ MO is a combination of the transition metal d_z^2 AO and the carbon 2s AO, causing this MO to be relatively energetically buried. Historically, the 1σ MO has been considered to be core-like and nonbonding in

character, but recent theoretical and experimental studies have revised this viewpoint, classifying it as a bonding orbital.[85-88] Now, molecules like RuC and its anionic analog are considered to have a quadruple bond in its ground electronic state because of the bonding character that has been recently identified in this 1σ MO.[85, 86] Next in energy is the degenerate pair of the bonding 1π MOs, which are comprised of ndπ AOs and 2pπ AOs of carbon. Following the 1π MOs is the 2σ MO which is a bonding combination of the transition metal d_z^2 AO and carbon's $2p_z$ and 2s AOs. For the neutral and cationic late MC molecules investigated in this study, the 1σ, 1π, and 2σ MOs are filled and additional electrons are placed in nonbonding orbitals, leading these molecules to be classified as quadruply bonded. Above these bonding MOs lie the degenerate pair of nonbonding 1δ MOs, which have nearly pure ndδ transition metal character because of the lack of low-lying δ orbitals on the carbon atom. Next in energy is the 3σ MO, which is a combination of the (n+1)*s* transition metal AO and the 2*p*σ AO of carbon. Akin to the 1σ MO, the character of the 3σ MO is currently debated in the literature. Previously, the 3σ MO was considered mainly transition metal in character with little contribution from the *p*-block constituent, leading to a nonbonding classification for the 3σ MO. However, it has been recently demonstrated for late MX compounds that electronic occupancies of the 3σ MO can be correlated to a decrease in the BDE for those molecules and the 3σ MO can be made up of nearly equal contributions from the transition metal and the *p*-block atom.[58, 89, 90] Accordingly, the 3σ orbital is now considered to be slightly antibonding in character. Finally, much higher in energy are the 2π and 4σ MOs, which are the antibonding counterparts of the 1π and 2σ MOs, respectively. The 2π and 4σ MOs are unoccupied in the neutral and cationic MCs investigated here.

B. RuC and RuC^+

Resonant two-photon ionization spectroscopic studies of RuC confirm that the ground state is $^1\Sigma^+$ ($1\sigma^2\ 1\pi^4\ 2\sigma^2\ 1\delta^4$).[23] The ground electronic state of the cation, RuC^+, has not been experimentally characterized, although previous calculations and our current calculations predict a $^2\Delta_{5/2}$ ($1\sigma^2\ 1\pi^4\ 2\sigma^2\ 1\delta^3$) ground state.[45] Upon ionization, the closed-shell RuC molecule ejects an electron from its nonbonding

metal-based 1δ MOs, giving RuC^+ its $^2\Delta_{5/2}$ electronic ground state. The energy required for ionization of a 1δ electron is assigned from Figure 1 as IE(RuC) = 7.439(40) eV. There are a handful of previous assignments for IE(RuC) in the literature, with the first coming from the R2PI spectroscopy study of RuC.[23] In that work, Langenberg *et al.* assigned IE(RuC) = 7.22(80) eV because RuC was not one-photon ionized by the 6.42 eV ionization laser employed in the experiments (this defined the lower limit) and the ν = 0 level of the $[12.7]^3\Pi_2$ state is the lowest observed excited state that could be ionized by the 6.42 eV ionization laser (this defined the upper limit). This error limit is quite large but nonetheless encompasses the IE(RuC) value reported here. Later, Shim and Gingerich reported mass spectrometric studies that used a linear extrapolation method to assign IE(RuC) = 8.4(7) eV,[91] which falls out of the range of our reported value. The ionization energy of RuC has also been calculated with density functional theory (DFT), where values of 7.59 eV and 7.67 eV were obtained.[92, 93] In the present work, we employed a CCSD(T)/CBSE methodology with a semi-empirical first-order spin-orbit correction procedure (See Section III) to calculate IE(RuC) = 7.48 eV, in good agreement with our measured value of IE(RuC) = 7.439(40) eV.

The ionization energy of RuC, 7.439(40) eV, exceeds that of atomic Ru, 7.36050(5) eV,[69] by only 0.079(40) eV. The thermochemical cycle given in Eqn. 1.1 demonstrates that D_0(RuC) must also exceed $D_0(Ru^+\text{-}C)$ by the same amount. Several previous experimental and theoretical studies have reported BDEs of RuC and RuC^+ that can be used with IE(Ru) and our value of IE(RuC) in Eqn. 1.1 to derive BDEs of RuC^+ and RuC. Three measurements of D_0(RuC) have been reported by Knudsen effusion mass spectrometry: 6.34(11) eV,[94] 6.68(13) eV,[95] and 6.55(13) eV.[56] Three previous measurements of $D_0(Ru^+\text{-}C)$ have also been reported by the Armentrout group using Guided Ion Beam Mass Spectrometry (GIBMS): 4.70(11) eV.[96] 6.27(15) eV,[97] and 5.43(8) eV.[45] If the IE(Ru), IE(RuC) and $D_0(Ru^+\text{-}C)$ = 5.43(8) eV are employed in Eqn. 1.1, D_0(RuC) = 5.51(9) eV is obtained. This value is at least 0.83 eV smaller than any of the Knudsen effusion measurements listed above. Moreover, it deviates significantly from a recent high-level calculation on D_0(RuC) that gives a BDE of 6.26 eV.[86] The GIBMS value of 4.70(11) eV is in even worse agreement with the Knudsen studies and the computational result. The GIBMS value of

$D_0(Ru^+\text{-}C)$ = 6.27(15) eV, however, leads to $D_0(RuC)$ = 6.35(16) eV, in much better agreement with the Knudsen effusion measurements and the computational study. The GIBMS measurements that yielded the smaller BDEs of RuC and RuC^+ investigated the reactions of Ru^+ with CH_4, C_2H_6, C_3H_8, and cyclopropane to form RuC^+, while the study that gave the larger value investigated the reaction of Ru^+ with CS_2 to form RuC^+. In the study that gave the larger value,[97] the authors point out that the earlier value of $D_0(Ru^+\text{-}C)$ = 4.70(11) eV, obtained by analysis of the cross-sections for the reaction of Ru^+ with cyclopropane and ethane, comes into agreement with the larger value, 6.27(15) eV, if the reactions studied produced different products than originally assigned. Thus, the complexity of the reactions of Ru^+ with hydrocarbons complicated the analysis of the reaction cross-section curves compared to the simpler reaction of $Ru^+ + CS_2 \rightarrow RuC^+ + S_2$. Therefore, we recommend $D_0(Ru^+\text{-}C)$ = 6.27(15) eV as the most reliable of the previously reported values. Conversely, if the previous Knudsen effusion measurement of $D_0(RuC)$ = 6.34(11) eV is employed in Eqn 1.1, a value of $D_0(Ru^+\text{-}C)$ = 6.26(12) eV is obtained. If the Knudsen measurement of $D_0(RuC)$ = 6.34(11) eV and the GIBMS result of $D_0(Ru^+\text{-}C)$ = 6.27(15) eV are employed in Eqn. 1.1, the two sides of the equation agree to within 0.01(19) eV. Because of this excellent agreement, we recommend $D_0(RuC)$ = 6.34(11) eV and $D_0(Ru^+\text{-}C)$ = 6.27(15) eV as the best currently available values. Table I summarizes previous experimental and computational results for IE(RuC), $D_0(RuC)$, and $D_0(Ru^+\text{-}C)$.

C. RhC and RhC^+

The $^2\Sigma^+$ ($1\sigma^2\ 1\pi^4\ 2\sigma^2\ 1\delta^4\ 3\sigma^1$) ground electronic state of RhC has been confirmed by numerous experimental studies.[24, 72, 98, 99] Although the ground electronic state of RhC^+ has not been experimentally determined, calculations in the current work and in the literature predict a $^1\Sigma^+$ ($1\sigma^2\ 1\pi^4\ 2\sigma^2\ 1\delta^4$) electronic ground state,[92] identical to the isoelectronic neutral molecule RuC. Our measurement in Figure 2 provides IE(RhC) = 7.458(32) eV, which is nearly identical with IE(Rh) = 7.45890(5) eV.[69] In atomic Rh, it is a 5s

electron that is removed upon ionization; in RhC it is the 3σ electron, which is primarily 5s in character. Thus, it makes sense that the IEs of Rh and RhC are similar.

Only two other measurements of IE(RhC) exist in the literature, obtained from the appearance potential of RhC^+ in Knudsen effusion mass spectrometry experiments.[55, 100] The first study gives IE(RhC) = 8.6(4) eV, more than 1 eV higher than our measured value.[55] The second study gives an appearance potential of 7.2(5) eV, in much closer agreement with our value of 7.458(32) eV. Using previous thermochemical data on the RhC and RhC^+ molecules and Eqn. 1.1, Hettich and Freiser derived IE(RhC) = 6.4(7) eV,[101] which underestimates our result. Previous DFT calculations of IE(RhC) range from 7.60 – 7.70 eV,[92, 93] 0.15 to 0.25 eV higher than our result. To rectify the lack of theoretical data on the IE(RhC), using the CCSD(T)/CBSE methodology we calculate a value of 7.47 eV for IE(RhC), in excellent agreement with our experimental IE(RhC) = 7.458(32) eV.

With this newly measured value for the IE of RhC, new values for the BDEs of RhC and RhC^+ can be derived using Eqn 1.1. There are three previously reported BDEs for RhC, all obtained from Knudsen effusion mass spectrometry. All of these results are very similar, providing BDEs for RhC of 5.97(4) eV,[36] 5.98(8) eV,[55] and 6.01(7) eV.[102] These give a weighted average of 5.98(3) eV. Using Eqn 1.1, and the values IE(RhC) = 7.458(32) eV, IE(Rh) = 7.45890(5) eV, and D_0(RhC) = 5.98(3) eV, a BDE for $D_0(Rh^+\text{-}C)$ = 5.98(4) eV is derived. Intriguingly, the value of $D_0(Rh^+\text{-}C)$ = 5.98(4) eV deviates greatly from previously reported measurements for the BDE of RhC^+. GIBMS has been used to measure $D_0(Rh^+\text{-}C)$ = 4.38(5) eV and $D_0(Rh^+\text{-}C)$ = 4.25(15) eV.[46, 103] In these studies, Rh^+ cations were collided with CH_4 [46] or with C_2H_6, C_3H_8, or cyclopropane.[103] As was found in the studies on Ru^+, the complexity of the reaction between Rh^+ and hydrocarbons apparently leads to a shift in the apparent threshold for RhC^+ production to higher collision energies, which falsely suggests a weak Rh^+-C bond. In another study, collisions of Rh^+ ions with toluene, cycloheptatriene, and norbornadiene were used to derive $D_0(Rh^+\text{-}C)$ = 7.09(69) eV.[104] Even with such a large error limit, this value is still significantly greater than the value derived from our measured IE(RhC) and the Knudsen effusion experiments.

Because of the consistency of the Knudsen effusion values of D_0(RhC) and the precision of the current result for IE(RhC), we recommend the weighted average value of the Knudsen effusion measurements, D_0(RhC) =5.98(3) eV and the associated cationic BDE of $D_0(Rh^+\text{-C})$ = 5.98(4) eV. In our opinion, these are the best values currently available for these thermochemical quantities. A summary of previous experimental and theoretical studies on $RhC^{0/+}$ is provided in Table II.

D. OsC and OsC^+

Akin to its isoelectronic 4d period neighbor RuC, the OsC molecule has also been studied using R2PI spectroscopy, where rotationally resolved spectra identified the ground state of OsC to be $^3\Delta_3$ arising from the $1\sigma^2\ 1\pi^4\ 2\sigma^2\ 1\delta^3\ 3\sigma^1$ configuration.[28] This differs from the $^1\Sigma^+$ ($1\sigma^2\ 1\pi^4\ 2\sigma^2\ 1\delta^4$) ground electronic state of isoelectronic RuC because the 6s orbital of Os is stabilized by relativistic effects,[105] causing preferential occupation of the 3σ orbital in OsC and the other 5d carbides. The OsC^+ molecule has not had its ground electronic state experimentally confirmed, but calculations for the present work as well as previously reported calculations predict a $^2\Delta_{5/2}$ ($1\sigma^2\ 1\pi^4\ 2\sigma^2\ 1\delta^3$) ground state for OsC^+.[48, 106] The low-lying $^4\Sigma^-$ ($1\sigma^2\ 1\pi^4\ 2\sigma^2\ 1\delta^2\ 3\sigma^1$) state is competitive for its ground state, but spin-orbit effects strongly stabilize the $^2\Delta_{5/2}$ ($1\sigma^2\ 1\pi^4\ 2\sigma^2\ 1\delta^3$) electronic state, making it the ground state.[48] Our measured IE(OsC) of 8.647(25) eV therefore corresponds to removal of the 3σ electron. There have been no previous measurements of the IE of OsC. The only previous value in the literature is a B3LYP calculation where IE(OsC) = 8.69 eV was obtained,[106] in good agreement with our measured value. In calculations for the present study, we used a CCSD(T)/CBSE methodology and semi-empirical spin-orbit corrections to obtain IE(OsC) = 8.62 eV, also in good agreement with our measured IE(OsC) = 8.647(25) eV.

Fewer experimental or computational studies have reported BDEs of OsC and OsC^+ than for the 4d MC molecules (M = Ru, Rh). A Knudsen effusion mass spectrometric study was used to obtain D_0(OsC) = 6.28(15) eV.[38] This may be converted to a BDE for Os^+-C using Eqn. 1.1 by using our measurement, IE(OsC) = 8.647(25) eV, and the literature value IE(Os) = 8.43823(20) eV.[69] This

procedure provides $D_0(Os^+\text{-}C) = 6.07(15)$ eV. This value is consistent with previous measurements of the OsC^+ BDE using GIBMS: 6.14(14) eV and 6.20(21) eV.[48, 107] We recommend a weighted average of these three values, giving $D_0(Os^+\text{-}C) = 6.13(9)$ eV. Inverting the calculation, the GIBMS values of $D_0(Os^+\text{-}C)$ may be combined with the ionization energies via Eqn. 1.1 to obtain $D_0(OsC)$ values of 6.35(14) and 6.41(21) eV. We recommend a weighted average of these values and the Knudsen effusion measurement, giving $D_0(OsC) = 6.34(9)$ eV. Table III provides a summary of previously reported experimental and computed values of IE(OsC), $D_0(OsC)$ and $D_0(Os^+\text{-}C)$.

E. IrC and IrC^+

The IrC molecule has been experimentally and theoretically confirmed to have a $^2\Sigma^+$ ($1\sigma^2\ 1\pi^4\ 2\sigma^2\ 1\delta^4\ 3\sigma^1$) ground electronic state.[82, 108, 109] The ground electronic state of IrC^+, however, has been up for debate in the literature.[48, 110] There are two competing possibilities: a $^1\Sigma^+$ ($1\sigma^2\ 1\pi^4\ 2\sigma^2\ 1\delta^4$) electronic state and a $^3\Delta_3$ ($1\sigma^2\ 1\pi^4\ 2\sigma^2\ 1\delta^3\ 3\sigma^1$) electronic state. Notably, these are the ground electronic states of isoelectronic RuC and OsC, respectively. Previous calculations performed by Kim *et al.* showed that both DFT and CCSD(T) calculations predict that the $^1\Sigma^+$ electronic state is the ground state of IrC^+, which matches the calculated results obtained in the present study.[48] However, when semi-empirical spin-orbit corrections are applied to the B3LYP calculations, the $^3\Delta_3$ electronic state is lowered below the $^1\Sigma^+$ electronic state and becomes the ground electronic state. The CCSD(T)/CBSE calculations of Kim *et al.*, however, still predict IrC^+ to have the $^1\Sigma^+$ ground electronic state even after the semi-empirical spin-orbit corrections are included.[48] Thus, the true electronic ground state of IrC^+ is ambiguous. In a recent review article concerned with the electronic structures and reactivities of transition metal and lanthanide atomic cations species, Armentrout asserts that the ground electronic state of IrC^+ is the $^1\Sigma^+$ electronic state,[111] in agreement with the CCSD(T)/CBSE results obtained here. Thus, the ionization of IrC corresponds to removal of the 6s-like 3σ electron. As displayed in Figure 4, we assign IE(IrC) = 8.933(74) eV.

To the best of our knowledge, only two previous measurements of IE(IrC) have been reported in the literature, both based on the appearance potential of IrC^+ in a Knudsen effusion mass spectrometry

experiment. Both studies report an appearance potential of 9.5(1.0) eV for IrC.[39, 56] Although this error limit is quite large, the reported value encompasses our more precise result. As in the case of OsC, Wang *et al.* used B3LYP to predict a value of 8.86 eV for IE(IrC),[106] in good agreement with our measured value. To compensate for the lack of higher-level computations on IrC, we calculated the IE of IrC with a CCSD(T)/CBSE methodology, giving IE(IrC) = 8.93 eV, in excellent agreement with the measured value of IE(IrC) = 8.933(74) eV.

Three Knudsen effusion investigations have been used to measure the BDE of IrC, obtaining 6.50(5) eV,[39] 6.47(11) eV,[112] and 6.43(13) eV.[56] These values for D_0(IrC) are also very similar to literature values for $D_0(Ir^+\text{-}C)$ obtained from GIBMS experiments: 6.58(12) eV and 6.59(5) eV.[48, 110] If the Knudsen values are combined with our measurement of IE(IrC) = 8.933(74) eV and the literature value IE(Ir) = 8.96702(22) eV,[69] $D_0(Ir^+\text{-}C)$ values of 6.53(9) eV, 6.50(13) eV, and 6.46(15) eV are obtained. These are in good agreement with the GIBMS result, so we recommend a value that is the weighted average of all five measurements: $D_0(Ir^+\text{-}C)$ = 6.56(4) eV. Inverting the procedure, the two GIBMS results may be converted to D_0(IrC) using Eqn 1.1 to give D_0(IrC) = 6.55(14) eV and 6.56(9) eV. Again, our recommended value is the result of a weighted average of all five results, giving D_0(IrC) = 6.50(4) eV. A summary of previous experimental and theoretical studies on $IrC^{0/+}$ is provided in Table IV.

F. PtC and PtC^+

Moving to PtC, the final electron is added to the 3σ MO, giving PtC its $^1\Sigma^+$ ($1\sigma^2\ 1\pi^4\ 2\sigma^2\ 1\delta^4\ 3\sigma^2$) ground state.[73, 113-115] As for the other MC^+ species noted here, the ground electronic state of PtC^+ has not been experimentally confirmed, but previous and current calculations show PtC^+ to have a $^2\Sigma^+$ ($1\sigma^2\ 1\pi^4\ 2\sigma^2\ 1\delta^4\ 3\sigma^1$) ground state.[106, 111] Therefore, the two-photon ionization threshold displayed in Figure 5, IE(PtC) = 9.397(32) eV, corresponds to removal of an electron from the 3σ MO. Notably, the IE of PtC is the largest of any of the MC species reported here and is nearly 2 eV greater than the IEs of RuC and RhC. Diatomic PtC is also the only late MC species investigated here for which a precise measurement of the IE has been previously reported. Unlike the low-precision values obtained from appearance potential

measurements, IE(PtC) has been measured by recording the photoionization efficiency curve of the jet-cooled molecule using tunable vacuum ultraviolet radiation produced at the Advanced Light Source at Lawrence Berkeley National Laboratory. Using this national facility, Citir *et al.* measured the IEs of PtC, PtO, and PtO_2,[54] obtaining IE(PtC) = 9.45(5) eV, in good agreement with the current measurement. The only other reported measurement of IE(PtC) comes from its appearance potential, measured in a Knudsen effusion mass spectrometry experiment, giving 9.5(1.0) eV.[39] A previous B3LYP calculation gave IE(PtC) = 9.39 eV,[106] also in good agreement with the present result. We have also computed the IE(PtC) using CCSD(T)/CBSE methods, obtaining IE(PtC) = 9.44 eV.

Previous measurements of D_0(PtC) and $D_0(Pt^+$-C) resemble the previously mentioned studies of the other late transition metal carbides, as they have been pursued using Knudsen effusion mass spectrometry for the neutrals and GIBMS for the cations. The three Knudsen effusion measurements of D_0(PtC) are all in close agreement with each other: 6.15(6) eV,[39] 6.27(11) eV,[112] and 6.30(7) eV.[102] These may be converted to values of $D_0(Pt^+$-C) using Eqn 1.1 with IE(PtC) = 9.397(32) eV from the present study and IE(Pt) = 8.95883(10) eV,[69] giving values of $D_0(Pt^+$-C) = 5.71(7) eV, 5.83(11) eV, and 5.86(8) eV. These are somewhat greater than the values reported in GIBMS experiments of $D_0(Pt^+$-C): 5.46(5) eV and 5.43(5) eV,[49, 116] implying a level of disagreement among the current measurements of these thermochemical properties. As the quoted uncertainties are similar for all five values, however, we have computed the weighted average of all five values to give a recommended value of $D_0(Pt^+$-C) = 5.57(9) eV. Inverting the procedure, the GIBMS results for $D_0(Pt^+$-C) lead to values of D_0(PtC) of 5.90(6) eV and 5.87(6) eV, respectively. These may be combined in a weighted average with the three Knudsen effusion values to obtain the recommended value of D_0(PtC) = 6.05(9) eV. For these recommended values, because the Knudsen effusion results and the GIBMS values lie outside of each other's error limits and are therefore inconsistent, we have used the reduced chi-squared to calculate the standard error of the weighted mean (variance weights, scale corrected) to estimate the error in the recommended value. A summary of previous experimental and theoretical studies on $PtC^{0/+}$ is provided in Table V.

G. Periodic Trends

Table VI lists the IEs of the transition metal atomic constituents of the MC molecules, the measured and calculated MC IEs from the current work, recommended MC and MC^+ BDEs, and the ground electronic configurations and term symbols of $RuC^{0/+}$, $RhC^{0/+}$, $OsC^{0/+}$, $IrC^{0/+}$, and $PtC^{0/+}$ along with other useful quantities to be discussed below. Overall, there is a general increase in the IEs for the late 4d and 5d MC species as their respective periods are traversed. The increase in IE going from RuC to RhC is slight, with the difference in their IEs being only 0.02(5) eV. The increase in IE across the late 5d MCs is more substantial, with a 0.29(8) eV increase between the IEs of OsC and IrC and an increase of 0.46(8) eV from IrC to PtC, giving an overall difference between the IEs of OsC and PtC of 0.75(4) eV. This nearly 1 eV difference between the IEs of the 5d MC species can be related to the differences between the IEs of the neutral transition metal atoms.

For most of the late MC molecules studied here, the IEs of the transition metal atoms are very similar to the IEs of the MC molecules themselves. For these molecules, the lowest ionization process corresponds to the removal of an electron from a transition metal-based 1δ or 3σ MO. This explains why the IEs of most of the MC species are very similar to the IEs of their respective transition metal constituents: IE(RuC) = 7.439(40) eV *vs.* IE(Ru) = 7.36050(5) eV; IE(RhC) = 7.458(32) eV *vs*. IE(Rh) = 7.45890(5) eV; IE(OsC) = 8.647(25) eV *vs*. IE(Os) = 8.43823(20) eV; and IE(IrC) = 8.933(74) eV *vs*. IE(Ir) = 8.96702(22) eV. For PtC, however, there is a significant discrepancy: IE(PtC) = 9.397(32) eV *vs*. IE(Pt) = 8.95883(10) eV. We would like to understand why PtC stands out as a unique case.

A more useful comparison might be to compare the ionization energy of the transition metal carbide with an atomic ionization process that corresponds to the removal of an electron from the atomic configuration and term that correlates to the electronic structure of the metal atom in the MC molecule. Likewise, the appropriate atomic ionization process should leave the M^+ ion in an electronic state that correlates to the ground electronic state of the MC^+ ion. The correlating states of the M and M^+ metal atoms may be determined by assuming that the 3σ orbital correlates to the metal atom (n+1)s orbital, that

the remaining valence electrons of the metal atom occupy the nd orbitals, and that the lowest energy term and level from this configuration correlates to the molecular state. Thus, for example, the $1\sigma^2\ 1\pi^4\ 2\sigma^2\ 1\delta^4\ 3\sigma^2$, $^1\Sigma^+$ ground state of PtC correlates to a $4d^8\ 5s^2$, $^3F_{4g}$ state of Pt, which lies at 823.6608 cm^{-1} or 0.102 eV.[69] Similarly, the $1\sigma^2\ 1\pi^4\ 2\sigma^2\ 1\delta^4\ 3\sigma^1$, $^2\Sigma^+$ ground configuration of PtC^+ correlates to a $4d^8\ 5s^1$, $^4F_{9/2g}$ state of Pt^+, which lies at 4786.6527 cm^{-1} or 0.593 eV.[69] It may be readily verified that the correlating states of the M atoms and M^+ ions that are so identified can combine with the C atom in its $^3P_{0g}$ ground level to form the ground electronic states of the MC and MC^+ molecules.[117] Having identified these correlating atomic states, it is appropriate to calculate the correlating IE of the metal atom using

$$\text{Correlating IE(M)} = \text{IE(M)} + \text{Correlating } M^+ \text{ term energy} - \text{Correlating M term energy} \qquad (5.2)$$

This equation provides the energy required to remove an electron from the atomic state that correlates to the ground state of the MC molecule and leaves the atomic ion in the state that correlates to the ground state of the MC^+ ion. In addition to the entries listed above, Table VI also provides the correlating electronic configurations and terms of the M atoms and M^+ ions, along with their energies. It also provides the result of the application of Eqn. 5.2, which gives the correlating ionization energy of the metal atom. Finally, the table lists the difference between the correlating IE(M) and the measured IE(MC) in the last row. Unfortunately, this procedure cannot be applied in the case of Os, because the electronic configurations of the known Os^+ atomic levels have not been identified.[69]

The correlating atomic ionization energy calculated for Rh using Eqn. (5.2) remains in good agreement with the measured IE(RhC) because the correlating atomic states of Rh and Rh^+ are still the ground states. The agreement is slightly worsened in the case of IrC, but the correlating IE(Ir) is still within 0.315 eV of IE(IrC). The agreement in the case of PtC is greatly improved, however, with the correlating IE(Pt) lying within 0.053 eV of the measured IE(PtC). As mentioned above, the procedure cannot be employed for Os because of poorly developed spectroscopic assignments for Os^+.

This procedure absolutely fails for RuC, however, leading to a difference between the modified IE(Ru) and IE(RuC) of over 1 eV. The problem is that the correlating state of atomic Ru, the $4d^8$, $^3F_{4g}$

state, lies quite high in energy, at 9120.63 cm^{-1}.[69] In the case of RuC, however, sufficient spectroscopic information is available to allow us to consider another ionization process. The ground state of RuC is the $1\sigma^2\ 1\pi^4\ 2\sigma^2\ 1\delta^4$, $^1\Sigma^+$ state, but the $1\sigma^2\ 1\pi^4\ 2\sigma^2\ 1\delta^3\ 3\sigma^1$, $^3\Delta_3$ state lies only 75.953 cm^{-1} higher in energy.[23] Can the correlating atomic IE approach provide a better approximation to the ionization energy of the low-lying $^3\Delta_3$ state? If so, this might help us to identify the problematic aspects of RuC. The ionization energy of the low-lying $^3\Delta_3$ state is reduced compared to that of the ground state by 75.953 cm^{-1} (0.009 eV), giving IE(RuC, $^3\Delta_3$) = 7.430(40) eV. The correlating Ru atom state for this configuration is the $4d^7\ 5s^1$, $^5F_{5g}$ term, which is the ground atomic state. As in the other examples, this term can combine with C $^3P_{0g}$ to produce the RuC $^3\Delta_3$ state.[117] Now, however, the correlating IE(Ru) requires no corrections and matches IE(Ru) exactly, as 7.36050(5) eV. This is in excellent agreement with the ionization energy of RuC in its $^3\Delta_3$ state, 7.430(40) eV.

The ionization processes for RuC($^3\Delta_3$), RhC, OsC, and PtC all involve simple loss of the (n+1)s-like 3σ electron. In these processes (omitting OsC, as explained above), the correlating atomic IE provides an excellent means of approximating the molecular IE, with deviations from the molecular IE below 0.07 eV. In IrC the ionization process is more complicated, removing a 3σ electron and dropping the remaining 3σ electron into the 1δ orbital. Even so, the discrepancy is only 0.315 eV. The $^1\Sigma^+$ ground state of RuC is unique in that it lacks 3σ electrons entirely and a 1δ electron is removed upon ionization. The close agreement between the correlating IE(M) and the molecular IE(MC) in cases where ionization is simply removal of a 3σ electron demonstrates that the 3σ orbital is primarily nonbonding in character.

The most perplexing question about RuC is why the $1\sigma^2\ 1\pi^4\ 2\sigma^2\ 1\delta^4$, $^1\Sigma^+$ state is the ground state at all. The configuration of bonding electrons in the $1\sigma^2\ 1\pi^4\ 2\sigma^2$ orbitals is the same as in the low-lying $1\sigma^2\ 1\pi^4\ 2\sigma^2\ 1\delta^3\ 3\sigma^1$, $^3\Delta_3$ state, but the $^3\Delta_3$ state correlates to ground state separated atoms while the $^1\Sigma^+$ state correlates diabatically to the Ru $4d^8$, $^3F_{4g}$ + C $2s^2\ 2p^2$, $^3P_{0g}$ excited separated atom limit at 9120.63 cm^{-1} (1.131 eV). This implies that the diabatic bond dissociation energy of the RuC $^1\Sigma^+$ ground state is 1.140 eV greater than that of the $^3\Delta_3$ state, even though the bonding portion of the electronic configuration

is identical. We have no answer to this conundrum but hope that this article will stimulate others to consider this question.

VI. CONCLUSION

The ionization energies of RuC, RhC, OsC, IrC, and PtC have been measured to good precision by the observation of the two-photon ionization thresholds of these molecules. For OsC, the present study provides the first experimental measurement, giving IE(OsC) = 8.647(25) eV. The IE(RuC) had been previously estimated by R2PI spectroscopy; the value of IE(RuC) = 7.439(40) eV reported in the current work reduces the uncertainty by a factor of 20. The only previous values for the IEs of RhC and IrC were obtained from appearance potentials in Knudsen effusion mass spectrometry experiments. For these two molecules, the current values of IE(RhC) = 7.458(32) eV and IE(IrC) = 8.933(74) eV reduce the error limits by an order of magnitude compared to their previous values, allowing for more precise information to be extracted about these molecules using thermochemical cycles. The current result of IE(PtC) = 9.397(32) eV is in good agreement with a previously reported value of IE(PtC) = 9.45(5) eV, confirming the validity of both measurements.[54] All of the IEs reported here for the RuC, RhC, OsC, IrC, and PtC molecules now meet the 3 kcal/mol or 0.13 eV experimental accuracy standard that has been suggested for transition metal containing compounds;[66] all except for IrC also meet the more stringent 1 kcal/mol standard originally put forward by John Pople.[65]

Previous measurements of the bond dissociation energies of the neutral MC molecules using Knudsen effusion mass spectrometry and of the cationic MC^+ molecules using guided ion beam mass spectrometry have been reviewed in light of the newly measured MC ionization energies and the thermochemical cycle that relates these values, Eqn. 1.1. Consistencies and inconsistencies have been noted and recommended BDEs of RuC, RhC, OsC, IrC, and PtC and their cations have been provided. We have previously employed a resonant three-photon ionization scheme to measure the BDE of VO to high accuracy (±0.002 eV)[118] and are currently in the process of measuring the BDEs of the late transition

metal carbides using this technique. We anticipate that these measurements will resolve the remaining inconsistencies for the BDEs of these species and their ions.

In this work, we have noted a close relationship between the ionization energies of the MC molecules and the corresponding transition metal atom and have introduced the concept of the correlating ionization energy of the metal atom. In this concept, the correlating state of the metal atom in both the neutral MC molecule and the MC cation is identified based on the number of electrons in the (n+1)s-like 3σ orbital, and the correlating ionization energy of the metal atom is the difference in energy between these correlating M and M^+ states. For RhC, IrC, and PtC, the correlating ionization energy of the metal atom is in good agreement with that of the transition metal carbide molecule. Similarly, for RuC in its low-lying $^3\Delta$ state, the correlating ionization atomic energy is also in excellent agreement with IE(RuC, $^3\Delta$). What remains unexplained is why the ground state of RuC is the $1\sigma^2\ 1\pi^4\ 2\sigma^2\ 1\delta^4$, $^1\Sigma^+$ state, rather than the $1\sigma^2\ 1\pi^4\ 2\sigma^2\ 1\delta^3\ 3\sigma^1$, $^3\Delta$ state, which correlates to a much lower-lying diabatic state of the separated atoms. It is our hope that this observation will stimulate further research on this issue.

ACKNOWLEDGEMENTS

The authors thank the National Science Foundation for their support of this research under Grant No. CHE-2305293. The authors also thank Kimberly H. Tomchak for helpful discussions regarding the derived MC and MC^+ bond dissociation energies and previous MC literature. We also thank Prof. Peter B. Armentrout for helpful discussions, particularly regarding the GIBMS measurements conducted in his group. The authors also express gratitude towards the Center for High Performance Computing at the University of Utah for their technical resources and support.

DATA AVAILABILITY

The data that support the findings of this study are available from the corresponding author upon reasonable request.

References:

[1]S. T. Oyama, in *The Chemistry of Transition Metal Carbides and Nitrides*, edited by S. T. Oyama (Springer Netherlands, Dordrecht, 1996), pp. 1-27.
[2]H. H. Hwu and J. G. Chen, Chem. Rev. **105,** 185-212 (2005).
[3]Q. Gao, W. Zhang, Z. Shi, L. Yang, and Y. Tang, Advanced Materials **31,** 1802880 (2019).
[4]C.-H. Jun, Chem. Soc. Rev. **33,** 610-8 (2004).
[5]D. Schröder, S. Shaik, and H. Schwarz, Acc. Chem. Res. **33,** 139-45 (2000).
[6]F. A. Cotton and G. Wilkinson, *Advanced Inorganic Chemistry*, 3rd ed. (Wiley, New York, 1972).
[7]Y. Xiao, J.-Y. Hwang, and Y.-K. Sun, Journal of Materials Chemistry A **4,** 10379-93 (2016).
[8]R. R. Schrock, Angewandte Chemie International Edition **45,** 3748-59 (2006).
[9]E.-i. Negishi, Angewandte Chemie International Edition **50,** 6738-64 (2011).
[10]G. Wilkinson, Science **185,** 109-12 (1974).
[11]C.-W. Chen, A. J. Merer, and Y.-C. Hsu, J. Mol. Spectrosc. **361,** 40-6 (2019).
[12]Z. Luo, H. Huang, Y.-C. Chang, Z. Zhang, Q.-Z. Yin, and C. Y. Ng, J. Chem. Phys. **141,** 144307 (2014).
[13]O. Krechkivska and M. D. Morse, J. Phys. Chem. A **117,** 13284-91 (2013).
[14]D. J. Brugh, M. D. Morse, A. Kalemos, and A. Mavridis, J. Chem. Phys. **133,** 034303 (2010).
[15]D. J. Brugh and M. D. Morse, J. Chem. Phys. **107,** 9772-82 (1997).
[16]A. G. Adam and J. R. D. Peers, J. Mol. Spectrosc. **181,** 24-32 (1997).
[17]D. J. Brugh and M. D. Morse, J. Chem. Phys. **117,** 10703-14 (2002).
[18]B. Simard, P. A. Hackett, and W. J. Balfour, Chem. Phys. Lett. **230,** 103-9 (1994).
[19]B. Suo and K. Balasubramanian, J. Chem. Phys. **126,** 224305 (2007).
[20]S. J. Rixon, P. K. Chowdhury, and A. J. Merer, J. Mol. Spectrosc. **228,** 554-64 (2004).
[21]Z. Luo, H. Huang, Z. Zhang, Y.-C. Chang, and C. Y. Ng, J. Chem. Phys. **141,** 024304 (2014).
[22]D. J. Brugh, T. J. Ronningen, and M. D. Morse, J. Chem. Phys. **109,** 7851-62 (1998).
[23]J. D. Langenberg, R. S. DaBell, L. Shao, D. Dreessen, and M. D. Morse, J. Chem. Phys. **109,** 7863-75 (1998).
[24]W. J. Balfour, S. G. Fougère, R. F. Heuff, C. X. W. Qian, and C. Zhou, J. Mol. Spectrosc. **198,** 393-407 (1999).
[25]J. D. Langenberg, L. Shao, and M. D. Morse, J. Chem. Phys. **111,** 4077-86 (1999).
[26]O. Krechkivska and M. D. Morse, J. Chem. Phys. **133,** 054309 (2010).
[27]S. M. Sickafoose, A. W. Smith, and M. D. Morse, J. Chem. Phys. **116,** 993-1002 (2002).
[28]O. Krechkivska and M. D. Morse, J. Chem. Phys. **128,** 084314 (2008).
[29]K. Jansson and R. Scullman, J. Mol. Spectrosc. **36,** 248 - 67 (1970).
[30]O. Appelblad, C. Nilsson, and R. Scullman, Phys. Scr. **7,** 65-71 (1973).
[31]A. Sevy, D. M. Merriles, R. S. Wentz, and M. D. Morse, J. Chem. Phys. **151,** 024302 (2019).
[32]A. Sevy, D. J. Matthew, and M. D. Morse, J. Chem. Phys. **149,** 044306 (2018).
[33]E. L. Johnson, Q. C. Davis, and M. D. Morse, J. Chem. Phys. **144,** 234306 (2016).
[34]D. J. Matthew, E. Tieu, and M. D. Morse, J. Chem. Phys. **146,** 144310 (2017).
[35]I. Shim, H. C. Finkbeiner, and K. A. Gingerich, J. Phys. Chem. **91,** 3171-8 (1987).
[36]I. Shim and K. A. Gingerich, J. Chem. Phys. **81,** 5937-44 (1984).
[37]A. Sevy, R. F. Huffaker, and M. D. Morse, J. Phys. Chem. A **121,** 9446-57 (2017).
[38]G. Meloni, L. M. Thomson, and K. A. Gingerich, J. Chem. Phys. **115,** 4496-501 (2001).
[39]S. K. Gupta, B. M. Nappi, and K. A. Gingerich, J. Phys. Chem. **85,** 971-6 (1981).
[40]D. E. Clemmer, J. L. Elkind, N. Aristov, and P. B. Armentrout, J. Chem. Phys. **95,** 3387-93 (1991).
[41]C. Angeli, G. Berthier, C. Rolando, M. Sablier, C. Alcaraz, and O. Dutuit, J. Phys. Chem. A **101,** 7907-13 (1997).
[42]C. L. Haynes, Y.-M. Chen, and P. B. Armentrout, J. Phys. Chem. **99,** 9110-17 (1995).
[43]M. R. Sievers and P. B. Armentrout, Organometallics **22,** 2599-611 (2003).

[44]M. R. Sievers, Y. M. Chen, C. L. Haynes, and P. B. Armentrout, Int. J. Mass Spectrom. **195,** 149-70 (2000).
[45]P. B. Armentrout and Y.-M. Chen, Int. J. Mass Spectrom. **413,** 135-49 (2017).
[46]Y.-M. Chen and P. B. Armentrout, J. Phys. Chem. **99,** 10775-9 (1995).
[47]C. S. Hinton, F. Li, and P. B. Armentrout, Int. J. Mass Spectrom. **280,** 226-34 (2009).
[48]J. Kim, R. M. Cox, and P. B. Armentrout, J. Chem. Phys. **145,** 194305 (2016).
[49]X.-G. Zhang and P. B. Armentrout, J. Phys. Chem. A **107,** 8904-14 (2003).
[50]Y. C. Chang, Z. Luo, Y. Pan, Z. Zhang, Y.-N. Song, S. Y. Kuang, Q. Z. Yin, K.-C. Lau, and C. Y. Ng, Phys. Chem. Chem. Phys. **17,** 9780-93 (2015).
[51]Y. C. Chang, C. S. Lam, B. Reed, K. C. Lau, H. T. Liou, and C. Y. Ng, J. Phys. Chem. A **113,** 4242-8 (2009).
[52]H. Huang, Y. C. Chang, Z. Luo, X. Shi, C.-S. Lam, K.-C. Lau, and C. Y. Ng, J. Chem. Phys. **138,** 094301 (2013).
[53]Y. C. Chang, X. Shi, K.-C. Lau, Q.-Z. Yin, H. T. Liou, and C. Y. Ng, J. Chem. Phys. **133,** 054310 (2010).
[54]M. Citir, R. B. Metz, L. Belau, and M. Ahmed, J. Phys. Chem. A **112,** 9584-90 (2008).
[55]D. L. Cocke and K. A. Gingerich, J. Chem. Phys. **57,** 3654-61 (1972).
[56]N. S. McIntyre, A. Vander Auwera-Mahieu, and J. Drowart, Trans. Faraday Soc. **64,** 3006 - 10 (1968).
[57]D. M. Merriles and M. D. Morse, J. Chem. Phys. **157,** 074303 (2022).
[58]D. M. Merriles, A. S. Knapp, Y. Barrera-Casas, A. Sevy, J. J. Sorensen, and M. D. Morse, J. Chem. Phys. **158,** 084308 (2023).
[59]B. K. Welch, N. M. S. Almeida, and A. K. Wilson, Mol. Phys.**,** e1963001 (2021).
[60]N. M. S. Almeida, T. R. L. Melin, S. C. North, B. K. Welch, and A. K. Wilson, J. Chem. Phys. **157,** 024105 (2022).
[61]Y. A. Aoto, A. P. de Lima Batista, A. Köhn, and A. G. S. de Oliveira-Filho, J. Chem. Theory Comput. **13,** 5291-316 (2017).
[62]J. Shee, B. Rudshteyn, E. J. Arthur, S. Zhang, D. R. Reichman, and R. A. Friesner, J. Chem. Theory Comput. **15,** 2346-58 (2019).
[63]D. Süß, S. E. Huber, and A. Mauracher, J. Chem. Phys. **152,** 114104 (2020).
[64]V. G. Solomonik and A. N. Smirnov, J. Chem. Theory Comput. **13,** 5240-54 (2017).
[65]J. A. Pople, Rev. Mod. Phys. **71,** 1267-74 (1999).
[66]N. J. DeYonker, K. A. Peterson, G. Steyl, A. K. Wilson, and T. R. Cundari, J. Phys. Chem. A **111,** 11269-77 (2007).
[67]D. J. Matthew and M. D. Morse, J. Chem. Phys. **138,** 184303 (2013).
[68]W. C. Wiley and I. H. McLaren, Rev. Sci. Instrum. **26,** 1150 - 7 (1955).
[69]A. Kramida, Yu. Ralchenko, J. Reader, and NIST ASD Team (2023). NIST Atomic Spectra Database (version 5.11), *https://physics.nist.gov/asd* (National Institute of Standards and Technology Gaithersburg, MD, 2022).
[70]Gaussian 16 Rev. B.01, M. J. Frisch, G. W. Trucks, H. B. Schlegel, G. E. Scuseria, M. A. Robb, J. R. Cheeseman, G. Scalmani, V. Barone, G. A. Petersson, H. Nakatsuji, X. Li, M. Caricato, A. V. Marenich, J. Bloino, B. G. Janesko, R. Gomperts, B. Mennucci, H. P. Hratchian, J. V. Ortiz, A. F. Izmaylov, J. L. Sonnenberg, Williams, F. Ding, F. Lipparini, F. Egidi, J. Goings, B. Peng, A. Petrone, T. Henderson, D. Ranasinghe, V. G. Zakrzewski, J. Gao, N. Rega, G. Zheng, W. Liang, M. Hada, M. Ehara, K. Toyota, R. Fukuda, J. Hasegawa, M. Ishida, T. Nakajima, Y. Honda, O. Kitao, H. Nakai, T. Vreven, K. Throssell, J. A. Montgomery Jr., J. E. Peralta, F. Ogliaro, M. J. Bearpark, J. J. Heyd, E. N. Brothers, K. N. Kudin, V. N. Staroverov, T. A. Keith, R. Kobayashi, J. Normand, K. Raghavachari, A. P. Rendell, J. C. Burant, S. S. Iyengar, J. Tomasi, M. Cossi, J. M. Millam, M. Klene, C. Adamo, R. Cammi, J. W. Ochterski, R. L. Martin, K. Morokuma, O. Farkas, J. B. Foresman, and D. J. Fox, Wallingford, CT, (2016).
[71]A. D. Becke, J. Chem. Phys. **98,** 5648-52 (1993).

[72]B. Kaving and R. Scullman, J. Mol. Spectrosc. **32,** 475 - 500 (1969).
[73]S. A. Beaton and T. C. Steimle, J. Chem. Phys. **111,** 10876-82 (1999).
[74]T. H. Dunning, Jr., J. Chem. Phys. **90,** 1007-23 (1989).
[75]R. A. Kendall, T. H. Dunning, and R. J. Harrison, J. Chem. Phys. **96,** 6796-806 (1992).
[76]D. Figgen, K. A. Peterson, M. Dolg, and H. Stoll, J. Chem. Phys. **130,** 164108 (2009).
[77]K. A. Peterson, D. Figgen, M. Dolg, and H. Stoll, J. Chem. Phys. **126,** 124101 (2007).
[78]K. A. Peterson, D. E. Woon, and T. H. Dunning, J. Chem. Phys. **100,** 7410-5 (1994).
[79]D. Feller, K. A. Peterson, and J. Grant Hill, J. Chem. Phys. **135,** 044102 (2011).
[80]D. M. Merriles, E. Tieu, and M. D. Morse, J. Chem. Phys. **151,** 044302 (2019).
[81]B. P. Pritchard, D. Altarawy, B. Didier, T. D. Gibson, and T. L. Windus, Journal of Chemical Information and Modeling **59,** 4814-20 (2019).
[82]H. Tan, M. Liao, and K. Balasubramanian, Chem. Phys. Lett. **280,** 219-26 (1997).
[83]D. M. Merriles, K. H. Tomchak, C. Nielson, and M. D. Morse, J. Am. Chem. Soc. **144,** 7557-61 (2022).
[84]D. M. Merriles, K. H. Tomchak, J. C. Ewigleben, and M. D. Morse, J. Chem. Phys. **155,** 144303 (2021).
[85]D. Tzeli, J. Comput. Chem. **42,** 1126-37 (2021).
[86]D. Tzeli and I. Karapetsas, J. Phys. Chem. A **124,** 6667-81 (2020).
[87]L. F. Cheung, T.-T. Chen, G. S. Kocheril, W.-J. Chen, J. Czekner, and L.-S. Wang, J. Phys. Chem. Lett. **11,** 659-63 (2020).
[88]G. Schoendorff, K. Ruedenberg, and M. S. Gordon, J. Phys. Chem. A **125,** 4836-46 (2021).
[89]L. F. Cheung, G. S. Kocheril, J. Czekner, and L.-S. Wang, J. Chem. Phys. **152,** 174301 (2020).
[90]J. M. Dore, A. G. Adam, D. W. Tokaryk, and C. Linton, J. Mol. Spectrosc. **360,** 44-8 (2019).
[91]I. Shim and K. A. Gingerich, Chem. Phys. Lett. **317,** 338-45 (2000).
[92]J. Wang, X. Sun, and Z. Wu, Chem. Phys. Lett. **426,** 141-7 (2006).
[93]B. Kharat, S. B. Deshmukh, and A. Chaudhari, Int. J. Quantum Chem. **109,** 1103-15 (2009).
[94]I. Shim, H. C. Finkbeiner, and K. A. Gingerich, The Journal of Physical Chemistry **91,** 3171-8 (1987).
[95]K. A. Gingerich, Chem. Phys. Lett. **75,** 523-6 (1974).
[96]P. B. Armentrout and Y. M. Chen, Journal of the American Society for Mass Spectrometry **10,** 821-39 (1999).
[97]P. B. Armentrout and I. Kretzschmar, Phys. Chem. Chem. Phys. **12,** 4078-91 (2010).
[98]J. M. Brom, Jr., W. R. M. Graham, and W. Weltner, Jr., J. Chem. Phys. **57,** 4116-24 (1972).
[99]X. Li and L.-S. Wang, J. Chem. Phys. **109,** 5264-8 (1998).
[100]K. A. Gingerich and S. K. Gupta, J. Chem. Phys. **69,** 505-11 (1978).
[101]R. L. Hettich and B. S. Freiser, J. Am. Chem. Soc. **109,** 3543-8 (1987).
[102]A. V. Auwera-Mahieu and J. Drowart, Chem. Phys. Lett. **1,** 311-3 (1967).
[103]Y.-M. Chen and P. B. Armentrout, J. Am. Chem. Soc. **117,** 9291-304 (1995).
[104]D. B. Jacobson, G. D. Byrd, and B. S. Freiser, Inorg. Chem. **23,** 553-7 (1984).
[105]J. P. Desclaux, At. Data Nucl. Data Tables **12,** 311 (1973).
[106]J. Wang, X. Sun, and Z. Wu, Journal of Cluster Science **18,** 333-44 (2007).
[107]P. B. Armentrout, L. Parke, C. Hinton, and M. Citir, ChemPlusChem **78,** 1157-73 (2013).
[108]A. J. Marr, M. E. Flores, and T. C. Steimle, J. Chem. Phys. **104,** 8183-96 (1996).
[109]H. F. Pang and A. S. C. Cheung, Chem. Phys. Lett. **471,** 194-7 (2009).
[110]F.-X. Li, X.-G. Zhang, and P. B. Armentrout, Int. J. Mass Spectrom. **255-256,** 279-300 (2006).
[111]P. B. Armentrout, Mass Spectrometry Reviews **41,** 606-26 (2022).
[112]K. A. Gingerich, Chem. Phys. Lett. **23,** 270-4 (1973).
[113]C. Qin, R. Zhang, F. Wang, and T. C. Steimle, Chem. Phys. Lett. **535,** 40-3 (2012).
[114]B. F. Minaev, Phys. Chem. Chem. Phys. **2,** 2851-6 (2000).
[115]T. C. Steimle, K. Y. Jung, and B.-Z. Li, J. Chem. Phys. **102,** 5937-41 (1995).
[116]X.-G. Zhang, R. Liyanage, and P. B. Armentrout, J. Am. Chem. Soc. **123,** 5563-75 (2001).
[117]G. Herzberg, *Molecular Spectra and Molecular Structure I. Spectra of Diatomic Molecules*, 2nd ed. (Van Nostrand Reinhold, New York, 1950).

[118]D. M. Merriles, A. Sevy, C. Nielson, and M. D. Morse, J. Chem. Phys. **153,** 024303 (2020).
[119]K. P. Jensen, J. Phys. Chem. A **113,** 10133-41 (2009).
[120]R. Guo and K. Balasubramanian, J. Chem. Phys. **120,** 7418-25 (2004).
[121]I. Shim and K. A. Gingerich, Surface Science **156,** 623-34 (1985).
[122]D. Süß, S. E. Huber, and A. Mauracher, The European Physical Journal D **73,** 135 (2019).

Table I. Previous work on the BDEs and IE values of $RuC^{0/+}$ [a]

RuC

Authors	IE(RuC) (eV)	Method	Year	Reference
Merriles *et al.*	**7.439(40)**	R2PI Spectroscopy	2023	This work
Merriles *et al.*	7.48	CCSD(T)/aug-cc-pVXZ(-PP) (X = T, Q, 5) CBSE	2023	This work
Kharat *et al.*	7.67	DFT	2009	93
Wang *et al.*	7.59	DFT	2006	92
Shim and Gingerich	8.4(7)	Linear Extrapolation	2000	91
Langenberg *et al.*	**7.22(80)**	R2PI Spectroscopy	1998	23
Authors	**D_0(RuC) (eV)**	**Method**	**Year**	**Reference**
Merriles *et al.*	6.34(11)	Recommended value; see Section V.B for details	2023	This work
Tzeli and Karapetsas	6.26	MRCISD+Q	2020	86
Jensen	6.28	DFT/TPSSh	2009	119
Kharat *et al.*	9.34 [b]	DFT	2009	93
Wang *et al.*	5.56	DFT	2006	92
Guo and Balasubramanian	6.60	FOCI	2004	120
Shim and Gingerich	5.53	Multi-Reference Configuration Interaction	2000	91
Shim *et al.*	**6.34(11)**	Knudsen Effusion Mass Spectrometry	1987	94
Shim and Gingerich	1.57	Configuration Interaction	1985	121
Gingerich	**6.68(13)**	Knudsen Effusion Mass Spectrometry	1974	95
McIntyre *et al.*	**6.55(13)**	Knudsen Effusion Mass Spectrometry	1968	56

RuC^+

Authors	$D_0(Ru^+-C)$ (eV)	Method	Year	Reference
Merriles *et al.*	6.27(15)	Recommended value; see Section V.B for details	2023	This work
Armentrout and Chen	**5.43(8)**	Guided Ion Beam Mass Spectrometry	2017	45
Armentrout and Kretzschmar	**6.27(15)**	Guided Ion Beam Mass Spectrometry	2010	97
Wang *et al.*	5.46	DFT	2006	92

Armentrout and Chen	**4.70(11)**	Guided Ion Beam Mass Spectrometry	1999	96
Langenberg *et al.*	6.45(81)	Derivation	1998	23

[a]**Bolded** values are assigned from experiment, regular type values are calculated.
[b]The authors reported a "binding energy", which is ambiguous as to whether D_e or D_0 was calculated.
[c]From Reference 69

Table II. Previous works on the BDEs and IE values of $RhC^{0/+}$ [a]

RhC

Authors	IE(RhC) (eV)	Method	Year	Reference
Merriles *et al.*	**7.458(32)**	R2PI Spectroscopy	2023	This work
Merriles *et al.*	7.47	CCSD(T)/aug-cc-pVXZ(-PP) (X = T, Q, 5) CBSE	2023	This work
Kharat *et al.*	7.76	DFT	2009	93
Wang *et al.*	7.63	DFT	2006	92
Hettich and Freiser	6.4(7)	Derivation	1987	101
Gingerich and Gupta	**7.2(5)**	Appearance Potential	1978	100
Cocke and Gingerich	**8.6(4)**	Appearance Potential	1972	55
Authors	**D_0(RhC) (eV)**	**Method**	**Year**	**Reference**
Merriles *et al.*	5.98(3)	Recommended value; see Section V.C for details	2023	This work
Kharat *et al.*	7.11 [b]	DFT	2009	93
Jensen	5.94	DFT/TPSSh	2009	119
Wang *et al.*	5.71	DFT	2006	92
Shim and Gingerich	1.53	Configuration Interaction	1985	121
Shim and Gingerich	**5.97(4)**	Knudsen Effusion Mass Spectrometry	1984	36
Cocke and Gingerich	**5.98(9)**	Knudsen Effusion Mass Spectrometry	1972	55
Auwera-Mahieu and Drowart	**6.01(7)**	Knudsen Effusion Mass Spectrometry	1967	102

RhC^+

Authors	$D_0(Rh^+-C)$ (eV)	Method	Year	Reference
Merriles *et al.*	5.98(4)	Recommended value; see Section V.C for details	2023	This work
Wang *et al.*	6.30	DFT	2006	92
Chen and Armentrout	**4.38(5)**	GIBMS	1995	46
Chen and Armentrout	**4.25(18)**	GIBMS	1995	103
Jacobson *et al.*	**7.09(69)**	Collision Induced Dissociation	1984	104

[a]**Bolded** values are assigned from experiment, regular type values are calculated.
[b]The authors reported a "binding energy", which is ambiguous as to whether D_e or D_0 was calculated

Table III. Previous works on the BDEs and IE values of $OsC^{0/+}$ [a]

OsC				
Authors	**IE(OsC) (eV)**	**Method**	**Year**	**Reference**
Merriles *et al.*	**8.647(25)**	R2PI Spectroscopy	2023	This work
Merriles *et al.*	8.62	CCSD(T)/aug-cc-pVXZ(-PP) (X = T, Q, 5) CBSE	2023	This work
Wang *et al.*	8.69	B3LYP	2007	106
Authors	**D_0(OsC) (eV)**	**Method**	**Year**	**Reference**
Merriles *et al.*	6.34(9)	Recommended value; see Section V.D for details	2023	This work
Jensen	6.77	DFT/TPSSh	2009	119
Wang *et al.*	5.93	B3LYP	2007	106
Meloni *et al.*	**6.28(15)**	Knudsen Effusion Mass Spectrometry	2001	38
OsC^+				
Authors	**$D_0(Os^+$-C) (eV)**	**Method**	**Year**	**Reference**
Merriles *et al.*	6.13(9)	Recommended value; see Section V.D for details	2023	This work
Kim *et al.*	**6.14(14)**	GIBMS	2016	48
Armentrout *et al.*	**6.20(21)**	GIBMS	2013	107
Wang *et al.*	6.19	B3LYP	2007	106

[a]**Bolded** values are assigned from experiment, regular type values are calculated.
[b]The authors reported a "binding energy", which is ambiguous as to whether D_e or D_0 was calculated.

Table IV. Previous works on the BDEs and IE values of $IrC^{0/+}$ [a]

IrC

Authors	IE(IrC) (eV)	Method	Year	Reference
Merriles *et al.*	**8.933(74)**	R2PI Spectroscopy	2023	This work
Merriles *et al.*	8.93	CCSD(T)/aug-cc-pVXZ(-PP) (X = T, Q, 5) CBSE	2023	This work
Wang *et al.*	8.86	B3LYP	2007	106
Gupta *et al.*	**9.5(1.0)**	Appearance Potential	1981	39
McIntyre *et al.*	**9.5(1.0)**	Appearance Potential	1968	56
Authors	**D_0(IrC) (eV)**	**Method**	**Year**	**Reference**
Merriles *et al.*	6.50(4)	Recommended value; see Section V.E for details	2023	This work
Jensen	6.59	DFT/TPSSh	2009	119
Wang *et al.*	6.36	B3LYP	2007	106
Gupta *et al.*	**6.50(5)**	Knudsen Effusion Mass Spectrometry	1981	39
Gingerich	**6.47(11)**	Knudsen Effusion Mass Spectrometry	1973	112
McIntyre *et al.*	**6.43(13)**	Knudsen Effusion Mass Spectrometry	1968	56

IrC^+

Authors	$D_0(Ir^+-C)$ (eV)	Method	Year	Reference
Merriles *et al.*	6.56(4)	Recommended value; see Section V.E for details	2023	This work
Kim *et al.*	**6.58(12)**	GIBMS	2016	48
Li *et al.*	**6.59(5)**	GIBMS	2006	110
Wang *et al.*	6.72	B3LYP	2007	106

[a]**Bolded** values are assigned from experiment, regular type values are calculated.
[b]The authors reported a "binding energy", which is ambiguous as to whether D_e or D_0 was calculated.

Table V. Previous works on the BDEs and IE values of $PtC^{0/+}$ [a]

PtC

Authors	IE(PtC) (eV)	Method	Year	Reference
Merriles *et al.*	**9.397(32)**	R2PI Spectroscopy	2023	This work
Merriles *et al.*	9.44	CCSD(T)/aug-cc-pVXZ(-PP) (X = T, Q, 5) CBSE	2023	This work
Citir *et al.*	**9.45(5)**	VUV Direct Photoionization	2008	54
Wang *et al.*	9.39	B3LYP	2007	106
Gupta *et al.*	**9.5(1.0)**	Appearance Potential	1981	39
Authors	**D_0(PtC) (eV)**	**Method**	**Year**	**Reference**
Merriles *et al.*	6.05(9)	Recommended value; see Section V.F for details	2023	This work
Süß *et al.*	6.39	CCSD(T)/def2-QZVP	2019	122
Jensen	6.42	DFT/TPSSh	2009	119
Wang *et al.*	5.86	B3LYP	2007	106
Gupta *et al.*	**6.15(6)**	Knudsen Effusion Mass Spectrometry	1981	39
Gingerich	**6.27(11)**	Knudsen Effusion Mass Spectrometry	1973	112
Auwera-Mahieu and Drowart	**6.30(7)**	Knudsen Effusion Mass Spectrometry	1967	102

PtC^+

Authors	$D_0(Pt^+-C)$ (eV)	Method	Year	Reference
Merriles *et al.*	5.57(9)	Recommended value; see Section V.F for details	2023	This work
Süß *et al.*	6.01	CCSD(T)/def2-QZVP	2019	122
Wang *et al.*	5.81	B3LYP	2007	106
Zhang and Armentrout	**5.46(5)**	GIBMS	2003	49
Zhang *et al.*	**5.43(5)**	GIBMS	2001	116

[a]**Bolded** values are assigned from experiment, regular type values are calculated.
[b]The authors reported a "binding energy", which is ambiguous as to whether D_e or D_0 was calculated

Table VI. Ionization Energies, Bond Dissociation Energies, and Ground Electronic States of $RuC^{0/+}$, $RhC^{0/+}$, $OsC^{0/+}$, $IrC^{0/+}$, and $PtC^{0/+}$

Property	RuC	RuC^+	RhC	RhC^+	OsC	OsC^+	IrC	IrC^+	PtC	PtC^+
IE(M) (eV) [a]	7.36050(5)		7.45890(5)		8.43823(20)		8.96702(22)		8.95883(10)	
IE(MC) (eV) [b]	7.439(40)		7.458(32)		8.647(25)		8.933(74)		9.397(32)	
IE(MC) (eV) (calculated) [c]	7.48		7.47		8.62		8.98		9.44	
IE(M)-IE(MC) (eV)	-0.079(40)		0.001(32)		-0.209(25)		0.034(74)		-0.438(32)	
Recommended D_0 (eV) [d]	6.34(11)	6.27(15)	5.98(3)	5.98(4)	6.34(9)	6.13(9)	6.50(4)	6.56(4)	6.05(9)	5.57(9)
$MC^{0/+}$ Ground Configuration[e]	$1\delta^4$	$1\delta^3$	$1\delta^4\ 3\sigma^1$	$1\delta^4$	$1\delta^3\ 3\sigma^1$	$1\delta^3$	$1\delta^3\ 3\sigma^2$	$1\delta^4$	$1\delta^4\ 3\sigma^2$	$1\delta^4\ 3\sigma^1$
$MC^{0/+}$ Ground Term[e]	$^1\Sigma^+$	$^2\Delta_{5/2}$	$^2\Sigma^+$	$^1\Sigma^+$	$^3\Delta_3$	$^2\Delta_{5/2}$	$^2\Delta_{5/2}$	$^1\Sigma^+$	$^1\Sigma^+$	$^2\Sigma^+$
$M^{0/+}$ ground Configuration [a]	$4d^7\ 5s^1$	$4d^7$	$4d^8\ 5s^1$	$4d^8$	$5d^6\ 6s^2$	$5d^6\ 6s^1$	$5d^7\ 6s^2$	$5d^7\ 6s^1$	$5d^9\ 6s^1$	$5d^9$
$M^{0/+}$ ground term [a]	$^5F_{5g}$	$^4F_{9/2g}$	$^4F_{9/2g}$	$^3F_{4g}$	$^5D_{4g}$	$^6D_{9/2g}$	$^4F_{9/2g}$	$^5F_{9/2g}$	$^3D_{3g}$	$^2D_{5/2g}$
Correlating $M^{0/+}$ configuration [a]	$4d^8$	$4d^7$	$4d^8\ 5s^1$	$4d^8$	$5d^7\ 6s^1$	$5d^7$	$5d^7\ 6s^2$	$5d^8$	$5d^8\ 6s^2$	$5d^8\ 6s^1$
Correlating $M^{0/+}$ term [a]	$^3F_{4g}$	$^4F_{9/2g}$	$^4F_{9/2g}$	$^3F_{4g}$	$^5F_{5g}$	$^4F_{9/2g}$	$^4F_{9/2g}$	$^3F_{4g}$	$^3F_{4g}$	$^4F_{9/2g}$
Correlating $M^{0/+}$ term energy (eV) [a]	1.131	0.00	0.00	0.00	0.638		0.00	0.281	0.102	0.593
Correlating IE(M) (eV) [f]	6.2297		7.4589				9.2476		9.4502	
Correlating IE(M) – IE(MC) (eV)	-1.209(40)		0.001(32)				0.315(74)		0.053(32)	

[a] From Reference 69

[b] Measured in the current work.

[c] Calculated with CCSD(T)/CBSE using aug-cc-pVXZ(-PP) (X = T, Q, 5) and, if applicable, a semi-empirical spin orbit stabilization correction (Section III).

[d] See Tables I - V and Section V.B – V.F for each recommended D_0 and their references.

[e] Calculated with B3LYP/aug-cc-pVQZ(-PP), experimental references from Section V.B. – V. F. In all cases the 1σ, 1π, and 2σ MOs are filled and are omitted from the table for clarity.

[f] Calculated as IE(M) + energy of correlating M^+ term – energy of correlating M term.

Figure Captions:

Figure 1. Two-photon ionization threshold in RuC (blue, upper trace) with the measured threshold at 29 975(150) cm^{-1} and the corresponding adiabatic ionization energy of IE(RuC) = 60 000(320) cm^{-1}. The atomic spectrum of Ru (red, bottom trace) was used for spectral calibration.

Figure 2. Two-photon ionization threshold in RhC (blue, upper trace) with the measured threshold at 30 050(120) cm^{-1} and the corresponding adiabatic ionization energy of IE(RhC) = 60 150(260) cm^{-1}. The atomic spectrum of Ru (red, bottom trace) was used for spectral calibration.

Figure 3. Two-photon ionization threshold in OsC (blue, upper trace) with the measured threshold at 34 845(90) cm^{-1} and the corresponding adiabatic ionization energy of IE(OsC) = 69 740(200) cm^{-1}. The atomic spectrum of Os (red, bottom trace) was used for spectral calibration.

Figure 4. Two-photon ionization threshold in IrC (blue, upper trace) with the measured threshold at 36 000(300) cm^{-1} and the corresponding adiabatic ionization energy of IE(IrC) = 72 050(600) cm^{-1}. The atomic spectrum of Ir (red, bottom trace) was used for spectral calibration.

Figure 5. Two-photon ionization threshold in PtC (blue, upper trace) with the measured threshold at 37 870(120) cm^{-1} and the corresponding adiabatic ionization energy of IE(PtC) = 75 790(260) cm^{-1}. The atomic spectrum of Os (red, bottom trace) was used for spectral calibration.

Figure 6. Qualitative Molecular Orbital diagram of RuC in its ground electronic $^1\Sigma^+$ state.

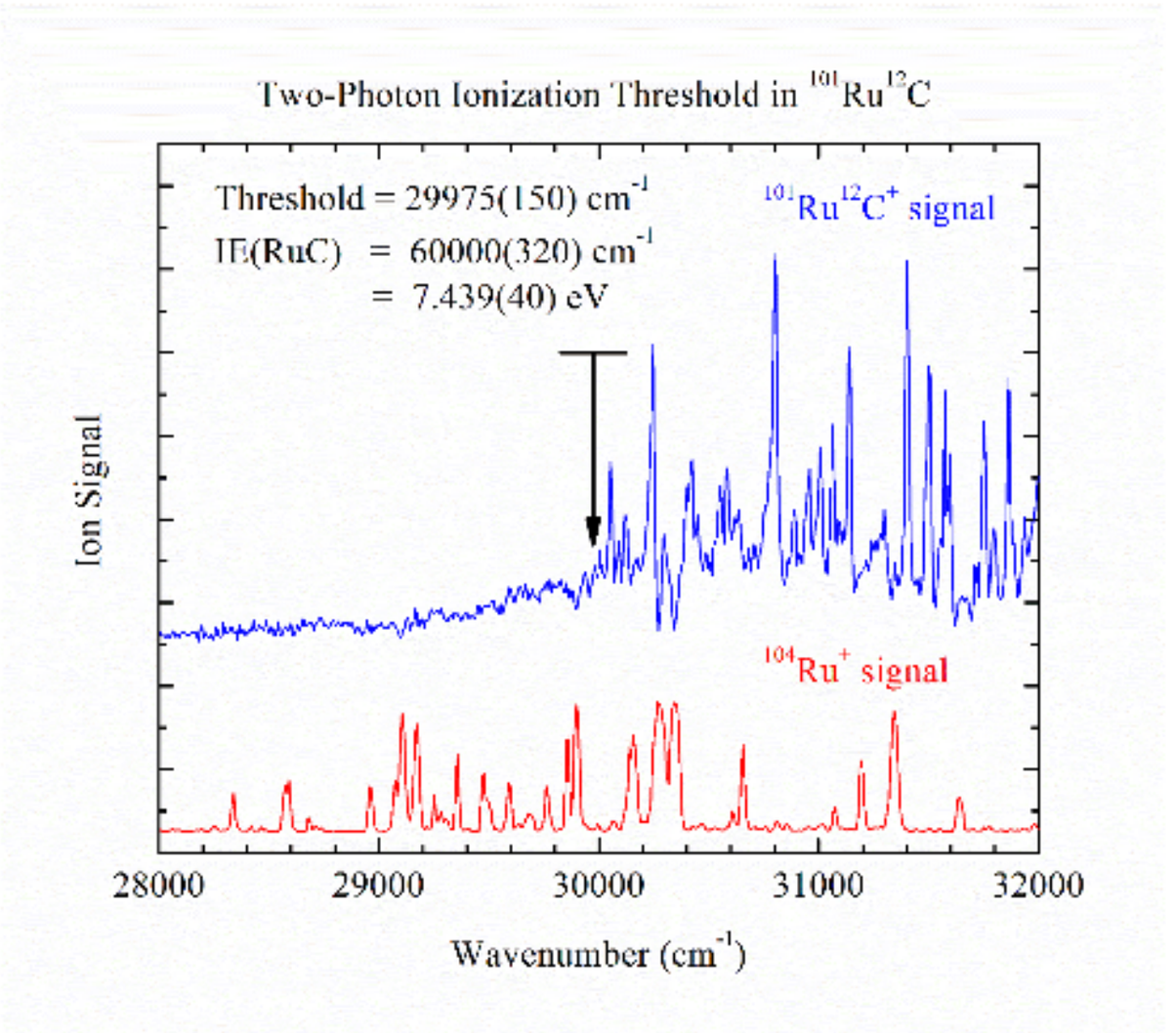

Figure 1. Two-photon ionization threshold in RuC (blue, upper trace) with the measured threshold at 29 975(150) cm^{-1} and the corresponding adiabatic ionization energy of IE(RuC) = 60 000(320) cm^{-1}. The atomic spectrum of Ru (red, bottom trace) was used for spectral calibration.

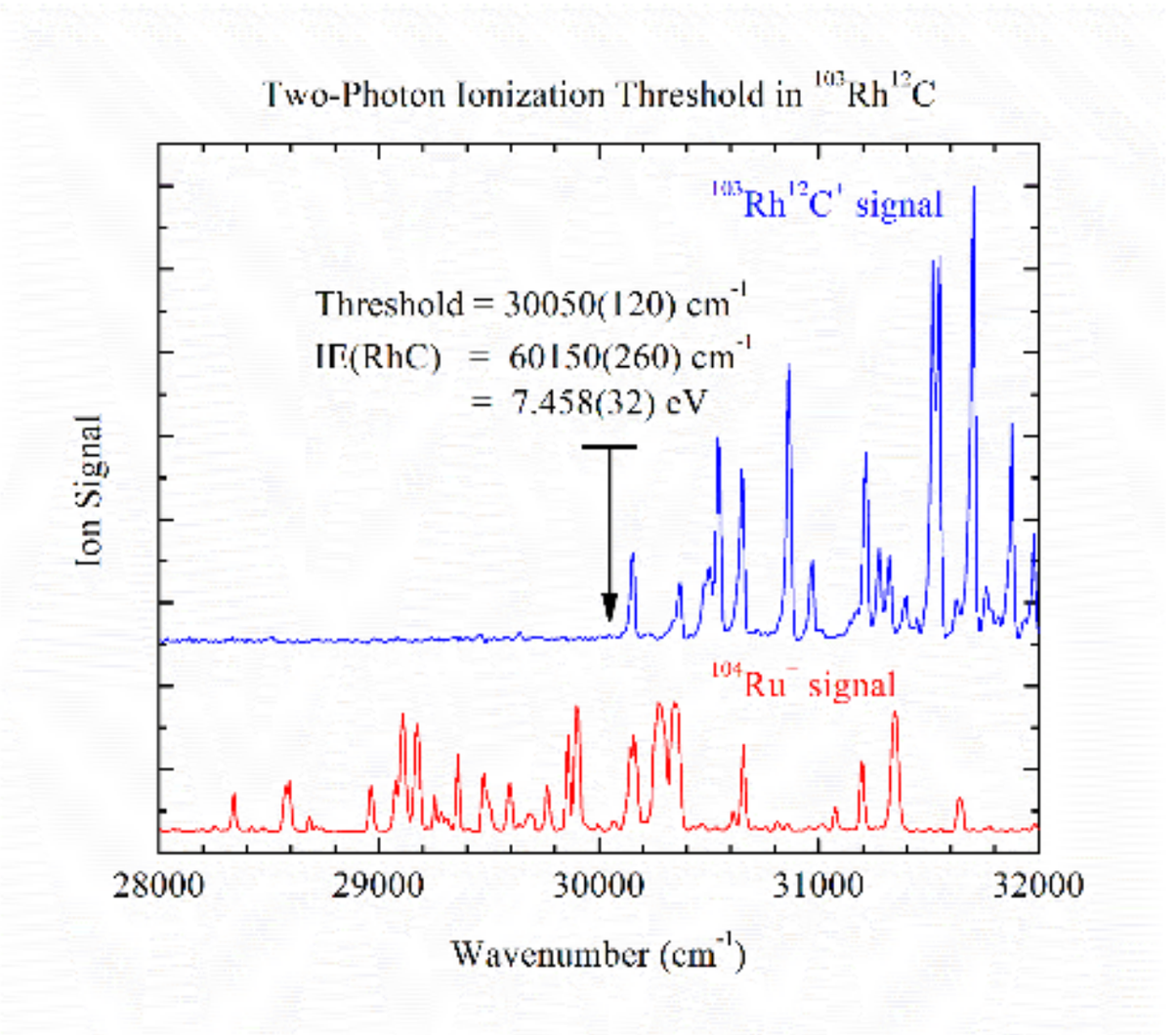

Figure 2. Two-photon ionization threshold in RhC (blue, upper trace) with the measured threshold at 30 050(120) cm^{-1} and the corresponding adiabatic ionization energy of IE(RhC) = 60 150(260) cm^{-1}. The atomic spectrum of Ru (red, bottom trace) was used for spectral calibration.

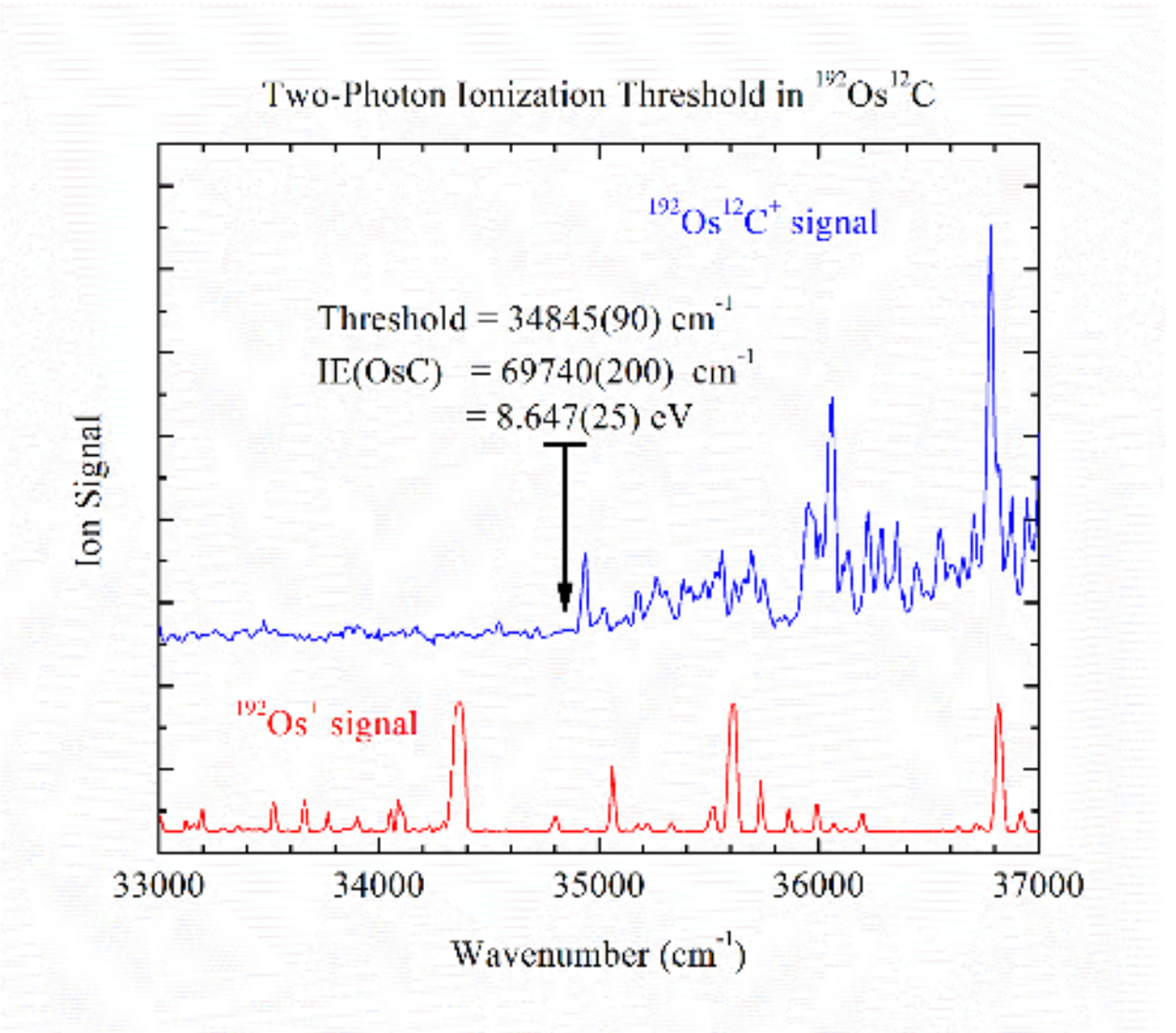

Figure 3. Two-photon ionization threshold in OsC (blue, upper trace) with the measured threshold at 34 845(90) cm^{-1} and the corresponding adiabatic ionization energy of IE(OsC) = 69 740(200) cm^{-1}. The atomic spectrum of Os (red, bottom trace) was used for spectral calibration.

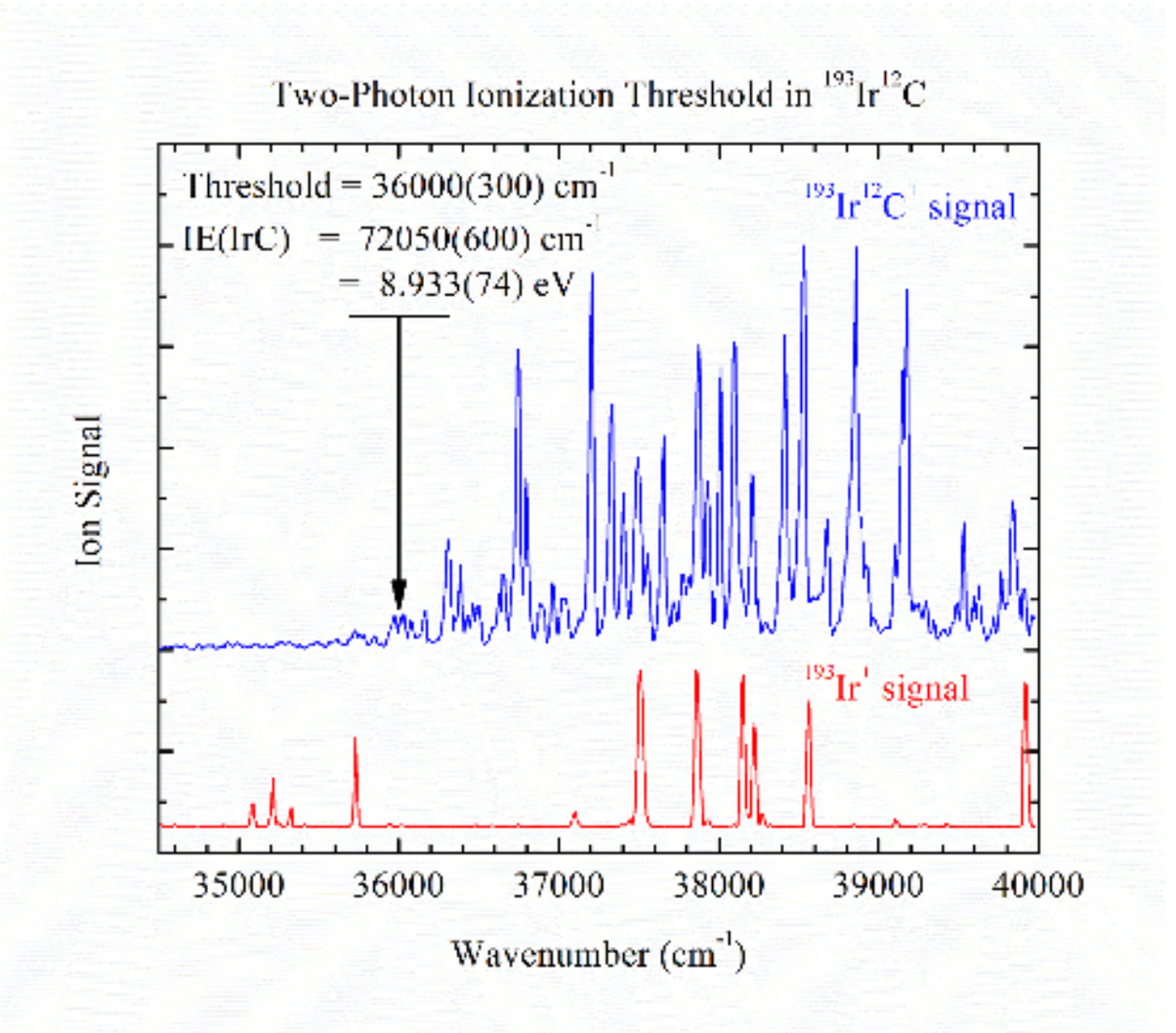

Figure 4. Two-photon ionization threshold in IrC (blue, upper trace) with the measured threshold at 36 000(300) cm^{-1} and the corresponding adiabatic ionization energy of IE(IrC) = 72 050(600) cm^{-1}. The atomic spectrum of Ir (red, bottom trace) was used for spectral calibration.

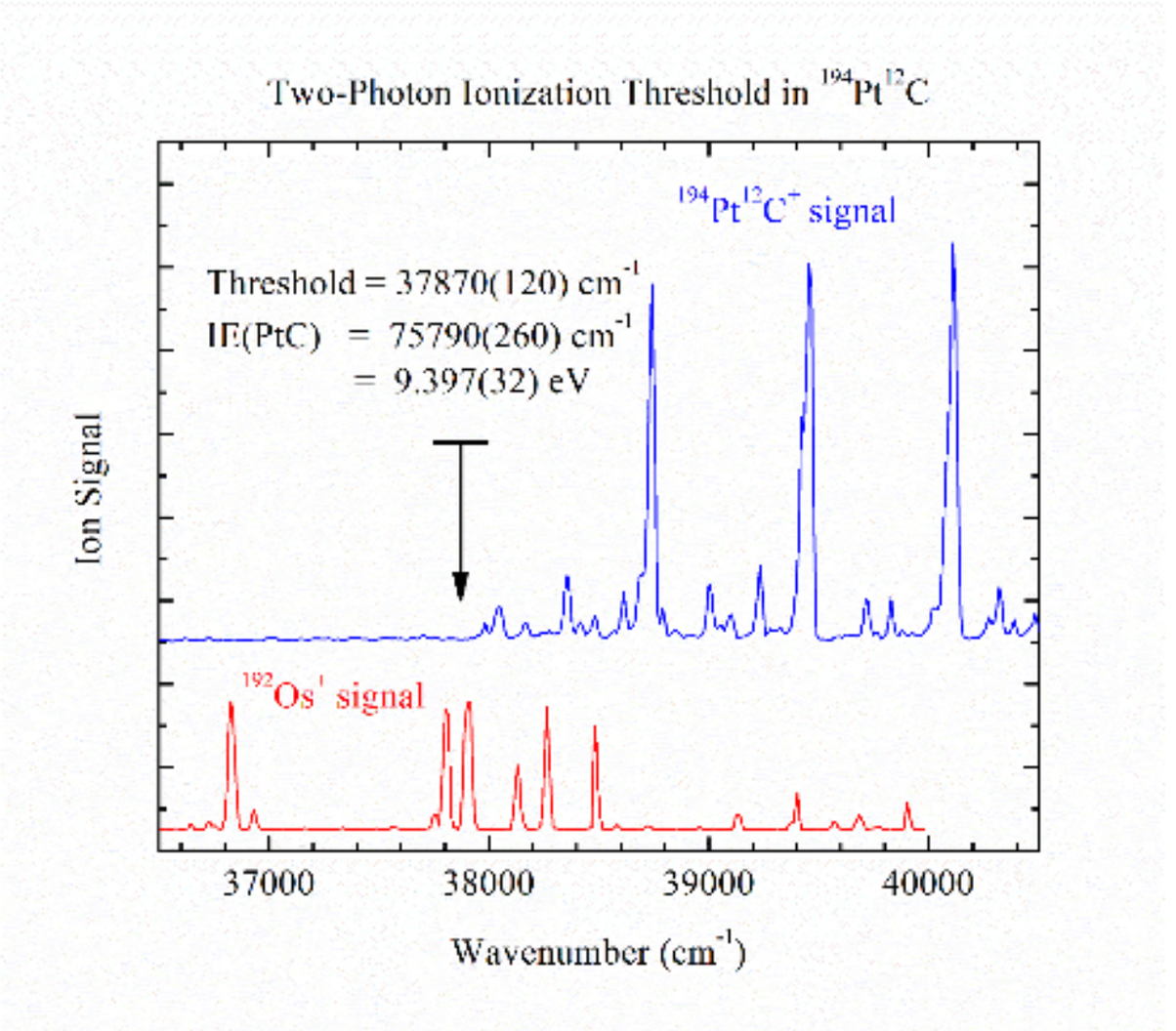

Figure 5. Two-photon ionization threshold in PtC (blue, upper trace) with the measured threshold at 37 870(120) cm^{-1} and the corresponding adiabatic ionization energy of IE(PtC) = 75 790(260) cm^{-1}. The atomic spectrum of Os (red, bottom trace) was used for spectral calibration.

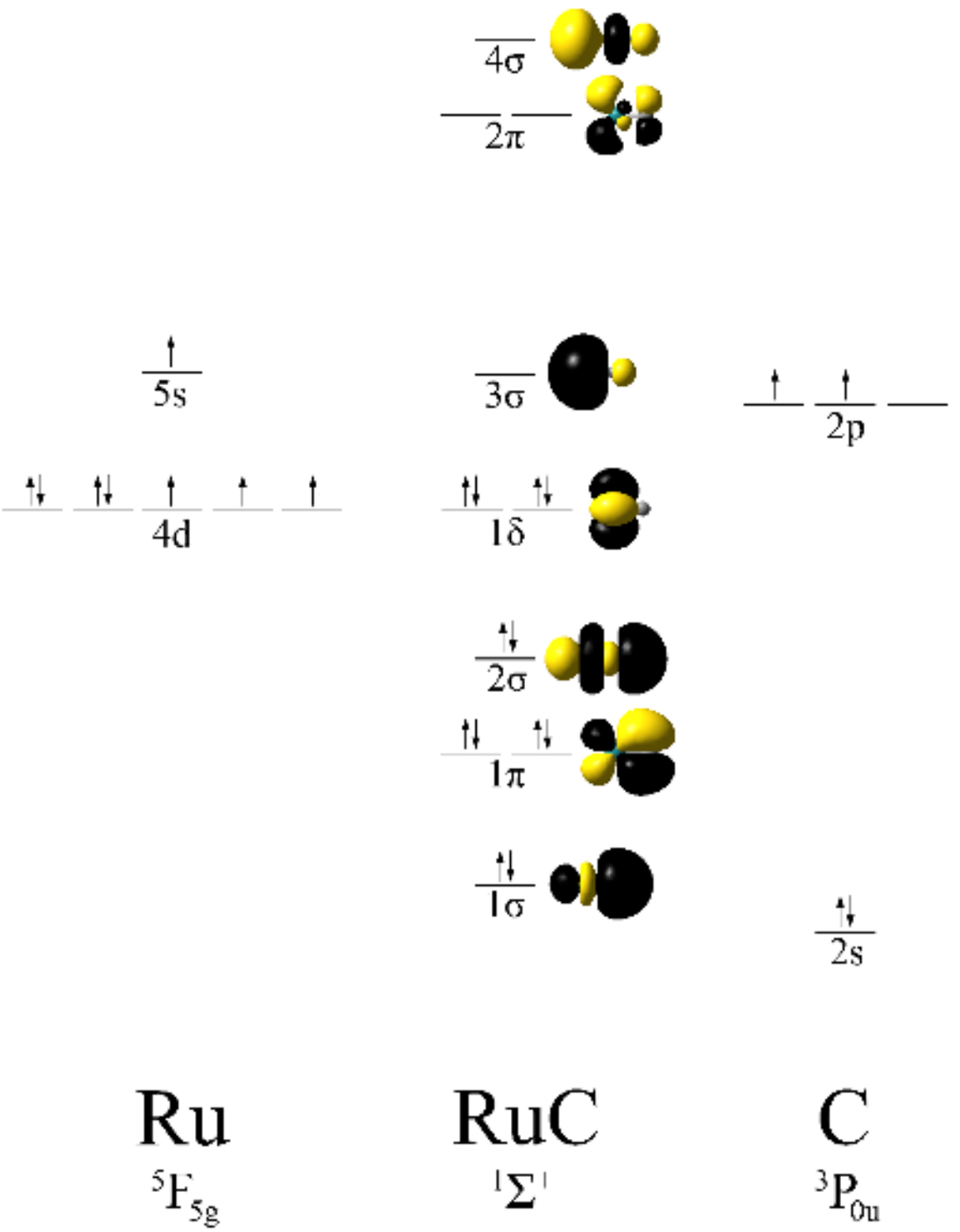

Figure 6. Qualitative Molecular Orbital diagram of RuC in its ground electronic $^1\Sigma^+$ state.